THE DETERMINATION OF OPTICAL PROPERTIES AND ENERGY GAP OF $Pb_{1-x}Sn_xTe$ THIN FILMS IN THE FUNDAMENTAL ABSORPTION EDGE REGION

Victor Martin Walz

NAVAL POSTGRADUATE SCHOOL
Monterey, California

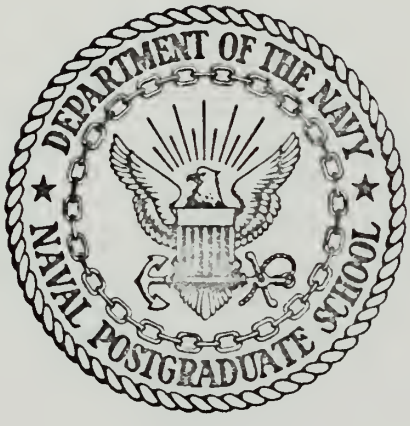

THESIS

The Determination of Optical Properties and Energy Gap of $Pb_{1-x}Sn_xTe$ Thin Films in the Fundamental Absorption Edge Region

by

Victor Martin Walz, Jr.

Thesis Advisor: Tien F. Tao

June 1972

The Determination of Optical Properties and Energy Gap of $Pb_{1-x}Sn_xTe$ Thin Films in the Fundamental Absorption Edge Region

by

Victor Martin Walz, Jr.
Ensign, United States Navy
B.S.E.E., Tulane University, 1971

Submitted in partial fulfillment of the
requirements for the degree of

MASTER OF SCIENCE IN ELECTRICAL ENGINEERING

from the

Naval Postgraduate School
June 1972

ABSTRACT

The optical properties of single-crystal $Pb_{1-x}Sn_xTe$ thin films in the fundamental absorption edge region were investigated. Tin compositions of $0 \leq x \leq 0.24$, where x is the mole fraction of SnTe, were studied from room to liquid nitrogen temperatures. Two thin film samples with $x = 0.70$ and $x = 0.85$ were also studied in an attempt to confirm the inversion of the conduction and valance bands which had been previously predicted for this narrow-gap semiconductor. The index of refraction n and the absorption coefficient α were determined from transmission and reflection measurements made on films 0.8 to 5.0 microns thick which were deposited on cleaved (100) faces of KCL rocksalt substrates. The optical energy gap was determined from the position of the absorption edge in the absorption spectrum.

The index of refraction was obtained using the interference fringe method. For $0 \leq x \leq 0.24$ a peak in n was observed. The index of refraction of films with a high Sn content exhibited free carrier absorption and free carrier concentration dependence. The absorption coefficient was calculated from an analysis of the theoretical reflectance R and transmittance T equations for a thin film on substrate model by using the experimentally determined R, T, and n values. The absorption spectrum showed relatively sharp absorption edges for $x \leq 0.24$ and broadened edges for higher Sn concentrations. Variations in the peak of the n spectra and the sharpness of the absorption edges were observed and accounted for.

TABLE OF CONTENTS

I. INTRODUCTION ---------- 9

A. OBJECTIVE OF THIS RESEARCH ---------- 9

B. THE NATURE OF $Pb_{1-x}Sn_xTe$ NARROW-GAP SEMICONDUCTORS--- 10

II. THEORETICAL ASPECTS ---------- 14

A. OPTICAL PROPERTIES AND ENERGY GAP OF SEMICONDUCTORS ---------- 14

1. Optical Properties from Electromagnetic Theory -- 14

2. The Experimental Parameters of Transmittance and Reflectance ---------- 18

B. THE DETERMINATION OF OPTICAL CONSTANTS AND ENERGY GAP ---------- 23

III. EXPERIMENTAL ASPECTS ---------- 26

A. PREPARATION AND CHARACTERIZATION OF $Pb_{1-x}Sn_xTe$ THIN FILMS ---------- 26

1. Growth of $Pb_{1-x}Sn_xTe$ Films ---------- 26

2. Film Analysis ---------- 26

B. REFLECTION AND TRANSMISSION MEASUREMENTS ---------- 29

1. Experimental Apparatus and Techniques ---------- 29

2. Experimental Results ---------- 40

C. DETERMINATION OF FILM THICKNESS ---------- 40

IV. RESULTS AND DISCUSSION ---------- 46

A. REFLECTANCE AND TRANSMITTANCE SPECTRA ---------- 46

B. OPTICAL CONSTANTS ---------- 52

1. The Index of Refraction ---------- 52

2. The Absorption Coefficient ---------- 60

C. THE ENERGY GAP ---------- 67

V. CONCLUSIONS ---------- 71

BIBLIOGRAPHY ---------- 72

INITIAL DISTRIBUTION LIST ---------- 74

FORM DD 1473 ---------- 75

LIST OF TABLES

TABLE

3-1 $Pb_{1-x}Sn_xTe$ Optical Samples Studied ---------- 27

3-2 Results of Film Thickness Measurements on the $Pb_{1-x}Sn_xTe$ Optical Samples Using the Scanning Electron Microscope ---------- 45

4-1 Energy Gap Data of $Pb_{1-x}Sn_xTe$ Alloys at Various Temperatures ---------- 68

LIST OF DRAWINGS

FIGURE

1-1 Energy Gap of $Pb_{1-x}Sn_xTe$ as a Function of x, the mole fraction of SnTe ---------- 12

1-2 Schematic representation of the valence and conduction bands at 12°K for PbTe for various compositions at which the energy gap is zero and for SnTe ---------- 13

2-1 Reflection and transmission of an electromagnetic wave at the boundary between two media ---------- 20

3-1 (a) Deposition System used in making $Pb_{1-x}Sn_xTe$ Optical Samples ---------- 28

(b) Laue picture of a $Pb_{1-x}Sn_xTe$ optical sample --------- 28

3-2 Typically prepared $Pb_{1-x}Sn_xTe$ thin film on a KCl substrate ---------- 30

3-3 (a) Spectrophotometer and low-temperature dewar in the trnasmission mode ---------- 31

(b) Low-temperature dewar assembly in sample beam ------- 31

3-4 (a) Low-temperature dewar assembly aligned for reflection measurements ---------- 32

(b) Beckman reflection assembly installed in sample area ---------- 32

3-5 Schematic diagrams of the transmission and reflection modes for the spectrophotometer ---------- 34

3-6 Schematic diagrams of low-temperature measurement techniques ---------- 35

3-7 Cross-section of cold finger and sample area inside vacuum enclosure ---------- 37

3-8 Typical spectrophotometer recording of reflection and transmission measurements ($Pb_{0.94}Sn_{0.06}Te$) ---------- 41

3-9 Calibration grid for the scanning electron microscope at 20K magnification ---------- 43

3-10 PbTe sample cross-section at 10K magnification ---------- 43

4-1 Typical thin-film reflectance and transmittance spectra ---------- 47

(a) x = 0.06, Film Thickness = 0.85, T = 300°K ---------- 47

(b) x = 0.06, Film Thickness = 0.85, T = 80°K ---------- 48

(c) x = 0.24, Film Thickness = 1.54, T = 300°K ---------- 49

(d) x = 0.70, Film Thickness = 1.27, T = 80, 300°K ------ 50

4-2 Index of Refraction spectra of single-crystal $Pb_{1-x}Sn_xTe$ Films ---------- 53

4-3 The index of refraction of single-crystal $Pb_{1-x}Sn_xTe$ films on rocksalt substrate compared with the results of Zemel, et.al., Reference 15 ---------- 61

4-4 Absorption Coefficients of $Pb_{1-x}Sn_xTe$ in the fundamental absorption edge region ---------- 62

4-5 Energy gap of $Pb_{1-x}Sn_xTe$ as a function of x, the mole fraction of SnTe determined experimentally from optical absorption ---------- 70

ACKNOWLEDGEMENTS

I would first like to thank Professor T. F. Tao under whose sincere guidance this thesis was made possible and Professor C.C. Wang for his numerous contributions in both the theoretical and experimental aspects of this research study. I am also deeply grateful to Raymond Zahm who prepared the optical samples analyzed in this study. I would also like to thank Professor John Schultz and Robert Sanders of the Department of Material Science and Chemistry who offered great assistance and advice in the operation of the Perkin-Elmer Spectrophotometer.

I would also like to thank the Office of Naval Research for their support in this research.

Finally, I would like to express my appreciation to Professor John Clarke and Roy Edwards for their assistance in the film x-ray analysis and characterization.

I. INTRODUCTION

A. OBJECTIVE OF THIS RESEARCH

The purpose of this research was to study the optical properties of ternary alloy $Pb_{1-x}Sn_xTe$ in the fundamental absorption region using reflection and transmission measurements performed on thin film samples.

$Pb_{1-x}Sn_xTe$ is a narrow-gap semiconductor whose energy gap is smaller than 0.33 eV and can be made to approach zero by changing the alloy composition x and temperature T. Consequently, it is an important semiconductor for generating and detecting infrared radiations of wavelengths larger than four microns. In the past four years, intensive efforts, supported by Department of Defense Agencies, have been given to developing $Pb_{1-x}Sn_xTe$ devices for passive infrared detection in reconnaissance and surveillance missions, and for active detection in CO_2 laser radar and communication systems. Recently, the Department of Transportation and major automobile corporations have become active in this research because $Pb_{1-x}Sn_xTe$ lasers and detectors are very useful as environmental pollution monitors. A coarse tuning laser within the infrared frequencies has been achieved by adjusting the chemical composition x which changes the energy gap of the semiconductor.

However, the optical properties of this promising semiconductor alloy system have hardly been studied. The optical properties that were determined in this study were the index of refraction, the absorption coefficient, and the optical energy gap. The variation of these properties with respect to Sn composition and temperature were analyzed. Of particular interest was the dispersion of the index of refraction in

the fundamental absorption region. The dispersion of n is an important parameter in determining the modes amplified by a semiconductor laser. The index of refraction as a function of wavelength was calculated using the interference fringe method and the experimentally obtained reflectance spectra. The absorption coefficients were determined using the transmittance, reflectance, and the index of refraction data. The optical energy gap was then obtained from the position of the calculated absorption edge. It was further attempted in this research to verify the experimental results to date which suggest that $Pb_{1-x}Sn_xTe$ alloys exhibit the inversion of conduction and valence bands [Refs. 1,2,3].

The optical energy gap for a limited number of compositions of $Pb_{1-x}Sn_xTe$ at liquid nitrogen temperatures and room temperatures have been previously determined from laser emission, photovoltaic effect, tunneling, and optical absorption [Refs. 2,3,4,5]. The variation of the energy gap with composition and temperature has also been quantitatively studied. This research of the optical properties of $Pb_{1-x}Sn_xTe$ gives new results on the optical constants and expands on the previous energy gap information.

B. THE NATURE OF $Pb_{1-x}Sn_xTe$ NARROW-GAP SEMICONDUCTORS

The IV-VI compound semiconductors PbTe and SnTe form pseudobinary solid solutions $Pb_{1-x}Sn_xTe$ with rocksalt structure [6]. Research to date has attempted to explain the composition dependence and temperature dependence of the energy gap. The change in energy gap E_g with composition for the $Pb_{1-x}Sn_xTe$ alloy series has been explained qualitatively in terms of the difference of relativistic effects in Pb and Sn. The observed behavior of the energy gap of $Pb_{1-x}Sn_xTe$ as a function of

composition x and temperature is shown in Figure 1-1 [2,3]. An energy band model proposed for $Pb_{1-x}Sn_xTe$, which describes the energy gap behavior is presented in Figure 1-2 [3]. It is known that the valence and conduction band edges in PbTe occur at the L point in the Brillouin zone. It is also known that the valence band-edge of PbTe is an L_6^+ state and the conduction band edge is an L_6^- state [7]. Increasing the Sn content results initially in a decrease in the energy gap as the L_6^+ and L_6^- states approach each other. At some intermediate composition where the two states become degenerate the energy gap goes to zero. Further increasing x causes the energy gap to increase with the L_6^+ state now forming the conduction band edge and the L_6^- state forming the valence band edge. Thus the bands have become inverted. For x greater than the intermediate composition where $E_g = 0$, the temperature dependence of the energy gap is of the opposite sign. The absolute magnitude of E_g increases with x and decreases with increasing temperature. Because the L_6^+ and L_6^- states each have only a two-fold spin degeneracy, this band inversion results in a semiconductor with the valence and conduction bands interchanged rather than a semimetal [3].

The IV-VI lead salt PbTe is a polar semiconductor with ten electrons in the unit cell and crystallizes in the cubic rocksalt structure. SnTe also crystallizes in the cubic rocksalt structure. These compounds form a complete series of pseudobinary solid solutions. Rocksalt structures are obtained for all values of x.

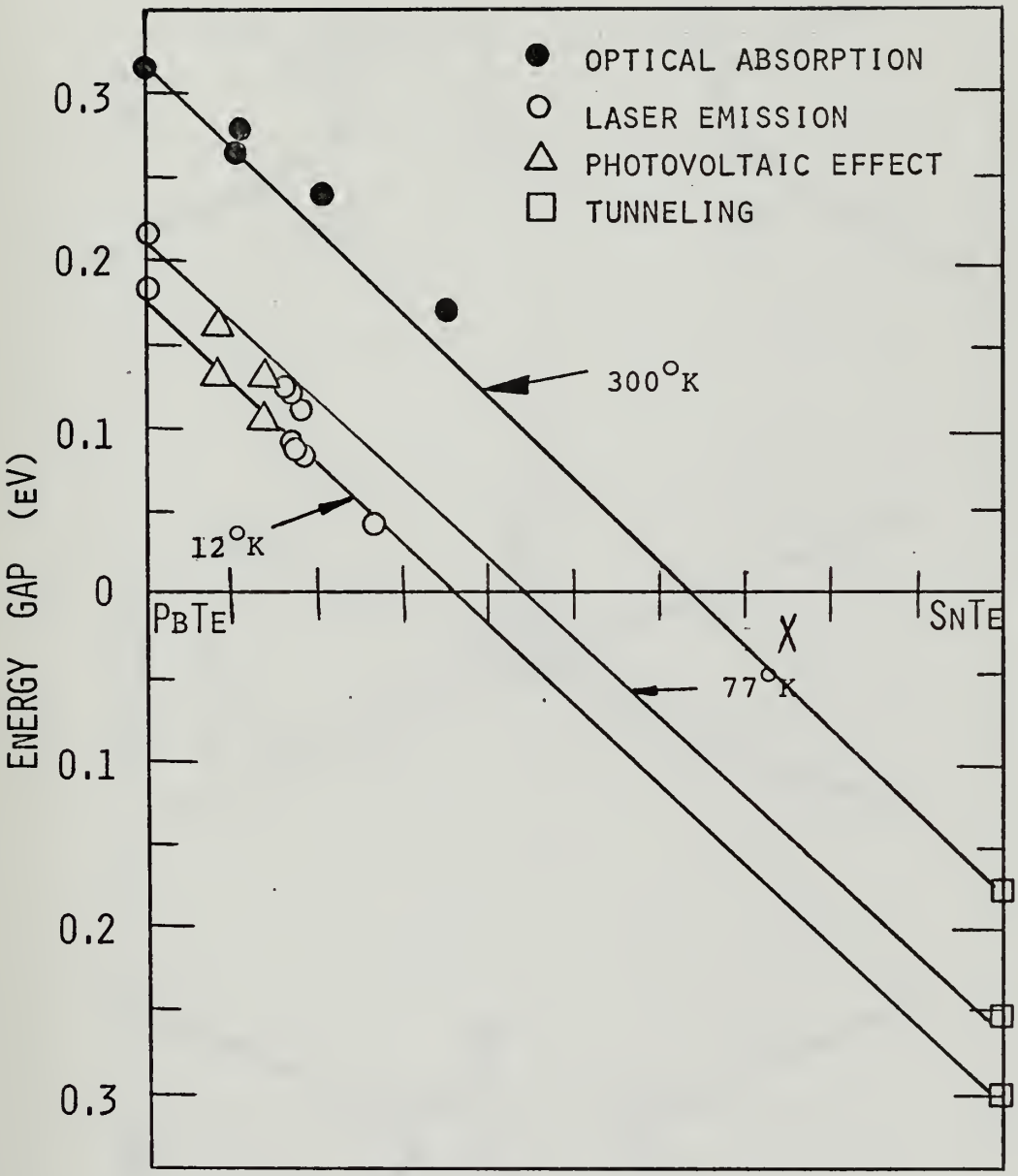

FIG. 1-1 - Energy gap of $Pb_{1-x}Sn_xTe$ as a function of x, the mole fraction of SnTe [2,3].

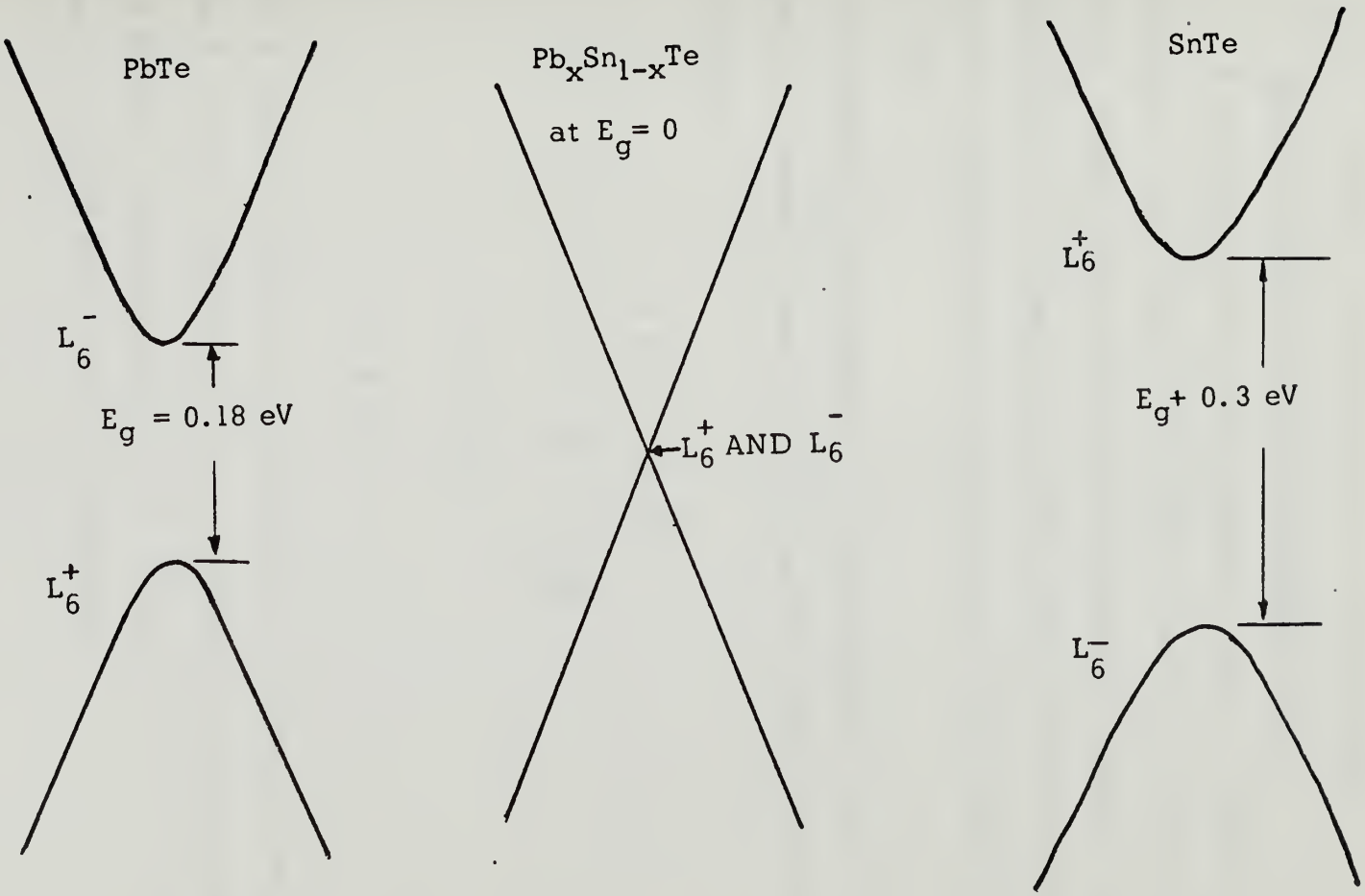

FIGURE 1-2

Schematic representation of the valence and conduction bands at 12°K for PbTe, for the composition at which the energy gap is zero, and for SnTe.

II. THEORETICAL ASPECTS

A. OPTICAL PROPERTIES AND ENERGY GAP OF SEMICONDUCTORS

1. Optical Properties from Electromagnetic Theory

A discussion of the electromagnetic theory of light in a conducting media is the basis of the optical properties studied in this research. Several authors have given a thorough treatment of this theory [8,9]. It is appropriate in this section to state the basic definitions and equations which are important in the study of $Pb_{1-x}Sn_xTe$ thin films.

The theory of the propagation of electromagnetic waves in conducting materials is based on Maxwell's field equations which may be written in CGS units as:

$$\nabla \times \overline{E} = -\frac{1}{c}\frac{\partial \overline{B}}{\partial t} \qquad (2\text{-}1a)$$

$$\nabla \times \overline{H} = \frac{4}{c}\overline{J} + \frac{1}{c}\frac{\partial \overline{D}}{\partial t} \qquad (2\text{-}1b)$$

$$\nabla \cdot \overline{D} = 4\pi\rho \qquad (2\text{-}1c)$$

$$\nabla \cdot \overline{B} = 0 \qquad (2\text{-}1d)$$

where $\overline{E}$ and $\overline{H}$ are the electric and magnetic field vectors respectively. $\overline{D}$ and $\overline{B}$ are their modifications by an intervening material medium, and $\overline{J}$ is the total current density. c is the speed of light. The material generates $\overline{D}$ and $\overline{B}$ from $\overline{E}$ and $\overline{H}$ in the manner:

$$J = \tilde{\sigma}\,\overline{E} \qquad (2\text{-}2a)$$

$$\overline{D} = \tilde{\varepsilon}\,\overline{E} \qquad (2\text{-}2b)$$

$$\overline{B} = \tilde{\mu}\,\overline{H} \qquad (2\text{-}2c)$$

where $\tilde{\sigma}$ is the conductivity tensor, $\tilde{\varepsilon}$ is the permittivity and $\tilde{\mu}$ is the permeability constant tensor. Equations (2-2) are valid for small magnitudes of $\bar{E}$ and $\bar{H}$.

From Equations (2-1) and (2) the wave equation for $\bar{E}$ and $\bar{H}$ can be derived as:

$$\left(\nabla^2 - \frac{4\pi\mu\sigma}{c^2}\frac{\partial}{\partial t} - \frac{\varepsilon\mu}{c^2}\frac{\partial^2}{\partial t^2}\right)\begin{matrix}\bar{E}\\ \bar{H}\end{matrix} = 0 \qquad (2\text{-}3)$$

where c is the velocity of light in a vacuum which is given by:

$$c = \frac{1}{\sqrt{\mu_o \varepsilon_o}} \qquad (2\text{-}4)$$

The plane wave solution to the wave equation has the form:

$$\bar{E} = \bar{E}_o \, e^{j\omega\left[t - \frac{\tilde{n}}{c}\,\bar{r}\cdot\bar{s}\right]} \qquad (2\text{-}5)$$

The plane waves of (2-5) are moving in a direction of $\bar{s}$ and $\tilde{n}$ is the complex index of refraction:

$$\tilde{n} = n - j\kappa = \frac{c}{v} \qquad (2\text{-}6)$$

The tilde symbol denotes a complex quantity. v is the velocity of wave propagation in the media. The wave solution can also be written as:

$$\bar{E} = \bar{E}_o \, e^{j(\tilde{k}\cdot r - \omega t)} \qquad (2\text{-}7)$$

where $\tilde{\kappa}$ is the complex wavevector and

$$\tilde{k} = \frac{\omega\bar{s}}{c}\,\tilde{n} \qquad (2\text{-}8)$$

Considering only a non-magnetic medium in which μ is unity, the plane wave solution can be substituted back into the wave equation (2-3) resulting in:

$$(n - j \kappa)^2 = \tilde{n}^2 = (\frac{c}{v})^2 = \tilde{\varepsilon} \qquad (2\text{-}10)$$

where $\tilde{\varepsilon}$ is the complex dielectric constant and $\tilde{n}$ is the complex index of refraction for an absorbing media. The n is the real part of the index of refraction, or simply the index of refraction, and κ is called the extinction coefficient. Rewriting the complex dielectric constant as:

$$\tilde{\varepsilon} = \varepsilon_1 + j\varepsilon_2 \qquad (2\text{-}11)$$

then:

$$\varepsilon_1 = n^2 - \kappa^2 \qquad (2\text{-}12a)$$

$$\varepsilon_2 = 2 n \kappa \qquad (2\text{-}12b)$$

The inverse equations for (2-12) are:

$$n = \left[\frac{\varepsilon_1}{2} + \frac{1}{2} (\varepsilon_1^2 - \varepsilon_2^2)^{\frac{1}{2}}\right]^{\frac{1}{2}} \qquad (2\text{-}13a)$$

$$\kappa = \left[-\frac{\varepsilon_1}{2} + \frac{1}{2} (\varepsilon_1^2 - \varepsilon_2^2)^{\frac{1}{2}}\right]^{\frac{1}{2}} \qquad (2\text{-}13b)$$

The sign choice in the root-taking process was governed by the requirement that κ be real and greater than zero and that $n \to \varepsilon_1^{\frac{1}{2}}$ as $\varepsilon_2 \to 0$. Collectively n and κ are termed the optical constants while ε_1 and ε_2 are termed the electromagnetic constants.

The interdependence of the real and imaginary parts of the complex optical parameters is expressed by the Kramers-Kronig relations, also

called the dispersion relations. For the complex index of refraction, $\tilde{n} = n(E) + j\,\kappa(E)$, as a function of the photon energy (E) the Kramers-Kronig relations give [9]:

$$\kappa(E) = \frac{2E}{\pi} \int_0^\infty \frac{n(E')\,dE'}{E^2 - E'^2} \tag{2-14a}$$

$$n(E) = 1 + \frac{2}{\pi} \int_0^\infty \frac{\kappa(E')E'\,dE'}{E'^2 - E^2} \tag{2-14b}$$

Thus if the index of refraction of a material is known for the total frequency spectrum or in the regions of dominant contribution, the extinction coefficient can be determined, or vice-versa. The dispersion analysis method is widely used in obtaining the optical constants of solids.

In optical studies the quantity which can be experimentally measured is the electromagnetic intensity which is proportional to the time average and vector magnitude of the Poynting vector as follows:

$$I = \left| \lim_{T\to\infty} \frac{1}{T} \int_0^T \frac{c}{4\pi} (\mathrm{Re}\,\bar{E} \times \mathrm{Re}\,\bar{H})\,dt \right| \tag{2-15}$$

which for plane waves of the form given by (2-5) propagating in the x direction becomes:

$$I \propto \frac{nc}{8\pi} E_o^2\, e^{-2\frac{\omega}{c}kx} = \frac{nc}{8\pi} E_o^2\, e^{-\left(\frac{4\pi\kappa}{\lambda}\right)x} \tag{2-16}$$

Thus in an absorbing medium the light intensity is attenuated by the factor:

$$e^{-\left(\frac{4\pi\kappa}{\lambda}\right)x}$$

where κ is the extinction coefficient. The factor $\frac{4\pi\kappa}{\lambda}$ is defined as the absorption coefficient α:

$$\alpha = \frac{4\pi\kappa}{\lambda} \tag{2-17}$$

The absorption coefficient is a very important parameter in understanding the absorption behavior of semiconductors. In this research, the variation of the absorption coefficient with wavelength is used to determine optical energy gap data. The fundamental absorption edge region has a sharp rise in the absorption coefficient in the photon energy spectrum.

The three very important optical parameters developed in this section were the index of refraction n, the extinction coefficient κ, and the absorption coefficient α.

2. The Experimental Parameters of Transmittance and Reflectance

The electromagnetic intensity is the experimentally measured parameter which was measured in this study. Electromagnetic radiation incident on a material is either transmitted or reflected with the remaining intensity attributed to absorption or light scattering due to surface or internal irregularities. The two fundamental experimentally measured parameters in optical studies are the transmittance T and the reflectance R. Transmittance is the ratio of the intensity of radiation emerging from a material to the intensity incident on the material. Reflectance is defined as the ratio of the intensity of electromagnetic radiation reflected from the material surface to the intensity incident on the surface of the material. Reflection occurs at the boundary between two media and is a function of the optical constants, angle of incidence, and the plane of polarization. If intensity losses due to scattering effects can be eliminated, then transmission and reflection measurements can yield useful information on the absorption behavior of the material. The radiation intensity incident on a material equals the intensities reflected, transmitted, and absorbed, if there are no losses.

Figure 2-1 describes the transmission and reflection phenomena for an electromagnetic wave at the boundary of two media. The relationship between the electromagnetic field vectors on each side of a discontinuity in the material medium are:

$$\bar{1} \cdot (\bar{B}_2 - \bar{B}_1) = 0 \qquad (2\text{-}18a)$$

$$\bar{1} \times (\bar{E}_2 - \bar{E}_1) = 0 \qquad (2\text{-}18b)$$

$$\bar{1} \times (\bar{H}_2 - \bar{H}_1) = j_s \qquad (2\text{-}18c)$$

$$\bar{1} \cdot (\bar{D}_2 - \bar{D}_1) = \rho_s \qquad (2\text{-}18d)$$

where 1 is the unit normal vector from medium 1 to medium 2, j_s is the surface current density, and ρ_s is the surface charge density. Both ρ_s and j_s are externally introduced quantities. In this optical study only radiation incident on boundaries where ρ_s and j_s are zero is considered. All optical measurements were taken at normal or near normal incidence so only the normal incidence case is considered.

The electromagnetic field vectors in each medium described in Figure 2-1 are:

$$E_1 = \bar{1}_y (E_i e^{\tilde{j}k_1 x} + E_r e^{-\tilde{j}k_1 x}) \qquad (2\text{-}19a)$$

$$H_1 = \bar{1}_z (H_i e^{\tilde{j}k_1 x} + H_r e^{-\tilde{j}k_2 x}) \qquad (2\text{-}19b)$$

$$E_2 = \bar{1}_y (E_t e^{\tilde{j}k_2 x}) \qquad (2\text{-}19c)$$

$$H_2 = \bar{1}_z (H_t e^{-\tilde{j}k_2 x}) \qquad (2\text{-}19d)$$

Since the electromagnetic intensity is a function of the electric field vector only, then the boundary condition of (2-18c) requires that:

$$E_t - E_i - E_r = 0 \qquad (2\text{-}20)$$

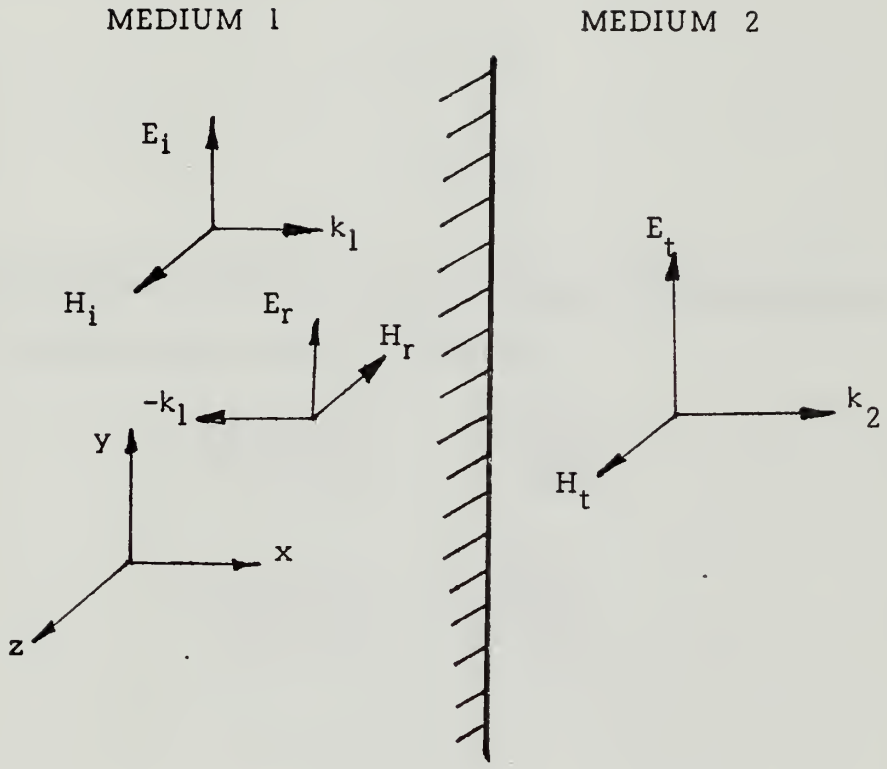

Figure 2-1

Reflection and Transmission of an
Electromagnetic Wave at the Boundary Between Two Media.

and

$$\tilde{k}_2 E_t - \tilde{k}_1 E_i - \tilde{k}_1 E_r = 0 \qquad (2\text{-}21)$$

The complex electric vector reflectance and transmittance coefficients are respectively defined as:

$$\rho = \frac{E_r}{E_i} \qquad (2\text{-}22a)$$

$$\tau = \frac{E_t}{E_i} \qquad (2\text{-}22b)$$

Combining Equations (2-20, 21, and 7) results in an expression for ρ and τ in terms of the index of refraction:

$$\rho = \frac{\tilde{\kappa}_1 - \tilde{\kappa}_2}{\tilde{\kappa}_1 + \tilde{\kappa}_2} = \frac{\tilde{n}_1 - \tilde{n}_2}{\tilde{n}_1 + \tilde{n}_2} \qquad (2\text{-}23a)$$

$$\tau = \frac{2\,\tilde{\kappa}_1}{\tilde{\kappa}_1 + \tilde{\kappa}_2} = \frac{2\,\tilde{n}_1}{\tilde{n}_1 + \tilde{n}_2} \qquad (2\text{-}23b)$$

and

$$\tau - \rho = 1 \qquad (2\text{-}24)$$

These expressions and boundary conditions which were developed for a two-media interface can be extended to media boundaries of multi-layered systems. In this study a $Pb_{1-x}Sn_xTe$ film on a KCL substrate was such a system.

The reflectance and transmittance parameters for the case of the thin absorbing film on a non-absorbing substrate of infinite thickness which were specifically applied in the study of $Pb_{1-x}Sn_xT_e$ are more complex owing to the increased number of media boundaries. The transmittance and reflectance equations for this case are given by [10, 11, 12]:

$$T = \frac{(n^2 + \kappa^2)n_s}{[(n+1)^2 + \kappa^2][(n+n_s)^2 + \kappa^2]}$$

$$\times \frac{16 \exp\left(-\frac{4\pi\kappa d}{\lambda}\right)}{1-2\, R_1R_2\exp\left(-\frac{4\pi\kappa d}{\lambda}\right) \cos\left(\frac{4\pi nd}{\lambda} + \delta_1+\delta_2\right) + R_1^2R_2^2 \exp\left(-\frac{8\pi\kappa d}{\lambda}\right)} \quad (2\text{-}25a)$$

$$R = \frac{R_1^2-2R_1R_2\exp\left(-\frac{4\pi\kappa d}{\lambda}\right) \cos\left(\frac{4\pi nd}{\lambda} - \delta_1+\delta_2\right) + R_2^2 \exp\left(-\frac{8\pi\kappa d}{\lambda}\right)}{1-2R_1R_2\exp\left(-\frac{4\pi\kappa d}{\lambda}\right)\cos\left(\frac{4\pi nd}{\lambda} + \delta_1+\delta_2\right) + R_1^2R_2^2\exp\left(-\frac{8\pi\kappa d}{\lambda}\right)} \quad (2\text{-}25b)$$

where: $R_1^2 = \frac{(n-1)^2 + \kappa^2}{(n+1)^2 + \kappa^2}$ $\qquad R_2^2 = \frac{(n-n_s)^2 + \kappa^2}{(n+n_s)^2 + \kappa^2}$

$$\delta_1 = \tan^{-1}\left(\frac{2\kappa}{n^2-1 + \kappa^2}\right) \qquad \delta_2 = \tan^{-1}\left(\frac{2n_s\kappa}{n^2-n_s^2 + \kappa^2}\right)$$

n = index of refraction of film

κ = extinction coefficient of film

n_s = index of refraction of substrate

d = thickness of film

δ_1 = phase angle occurring at the air-film interface

δ_2 = phase angle occurring at the film-substrate interace.

This case of thin absorbing film on a non-absorbing substrate of infinite thickness is a very good approximation of the situation of a $Pb_{1-x}Sn_xTe$ thin film on a substrate of finite thickness. Equations (2-25) are much simpler than similar expressions in which the thickness of the substrate is taken to be finite. Equations (2-25) are particularly applicable to films of thicknesses less than a few microns and have been successfully and widely used in thin film optical studies [13].

Equations (2-25) take into account the constructive and destructive interference phenomena which may occur in the films. In spectral regions, where the semiconductor film is transparent, the interference phenomena produces oscillating fringes. The maxima and minima of these finges are given by the normal incidence interference relation:

$$m\lambda_m = 2\,n\,d \qquad m = \frac{1}{2},\ 1,\ 1\,\frac{1}{2},\ 2,\ldots. \tag{2-26}$$

where n is the index of refraction of the film, and d is the film thickness, λ is the wavelength in free space, and m is the fringe order. The order is an integer for maxima and a half-integer for minima for transmission spectra and vice-versa for reflectance spectra. In order that the interference phenomena may produce pronounced maxima and minima, the film must have a sharply defined thickness. The interference relation takes into account the usual phase change of 180° between light reflected from the front and back surfaces of the film.

Equations (2-25) and (2-26) were the important theoretical relations utilized in the optical studies of $Pb_{1-x}Sn_xTe$.

B. THE DETERMINATION OF OPTICAL CONSTANTS AND ENERGY GAP

The optical studies of $Pb_{1-x}Sn_xTe$ were conducted by obtaining transmittance and reflectance spectral information in the region of the fundamental absorption edge. This R and T data combined with the theoretical relations for R and T (2-25) can be used to determine the index of refraction n and the extinction coefficient κ. The theoretical R and T equations cannot be solved explicitly for n and κ of the films in terms of the experimental values of R and T. Equations (2-25) also

admit more than one solution for n and κ for given values of R and T. Determination of n and κ from the R-T equations thus requires an initial guess of n and κ which must be adjusted until the best agreement is obtained with the experimentally measured reflectance and transmittance. A computer iterative search procedure was thus used in solving the R-T equations.

Since the index of refraction in the solution of the R-T equations is very sensitive to small errors in R and T, the R-T equations were used to determine only the extinction coefficient κ. The refractive index was determined independently using the interference fringe condition given by Equation (2-26). This relation requires knowledge of the film thickness d and the fringe order m. The fringe order m was assigned unambiguously by determining the wavelengths of the minima or maxima of at least two successive low-order fringes by making a rough estimate of the wavelength dependence of n and by applying Equation (2-26) [17, 18], and then applying:

$$\frac{m}{m+1} = \frac{\lambda_{m+1}\, n(\lambda_m)}{\lambda_m\, n(\lambda_{m+1})} \qquad (2\text{-}27)$$

The accuracy in determining the index of refraction using the interference fringe method essentially depends on the accuracy of the thickness determination. This particular aspect of this research will be discussed in the next section.

The values of n as a function of wavelength which have been determined independently of the R-T relations can then be substituted into the R-T equations resulting in only one variable κ to fit the experimentally determined R and T. The only approximation which must be true is that $(n-1)^2 > \kappa^2$ which seems to be applicable to $Pb_{1-x}Sn_xTe$ films.

The absorption spectra determined from the calculated absorption coefficients in the above manner is relatively insensitive to errors in R, T, and n.

The behavior of the absorption spectra in the fundamental absorption region can yield information on the energy gap of the semiconductor. There are a number of methods by which the indirect and direct optical energy gap can be derived from absorption coefficient data. However, some methods require accurate absorption coefficients in the higher energy region above the absorption edge where α begins to level off. The optical energy gap of direct gap semiconductors can be defined in several ways. It is often defined to be the photon energy corresponding to an arbitrary α value such as 10^3 (cm^{-1}) at the absorption edge. Another accepted method of determining the energy gap involves choosing a range of photon energies corresponding to a range in α thus revealing the sharpness in the absorption edge, and defining the optical energy gap to be the photon energy corresponding to $\frac{1}{2}\alpha_o$ where α_o is the value at the knee region above the absorption edge. This definition of the optical energy gap was used in this study of $Pb_{1-x}Sn_xTe$ which exhibits strong evidence of direct energy gap transition [1,2].

III. EXPERIMENTAL ASPECTS

A. PREPARATION AND CHARACTERIZATION OF $Pb_{1-x}Sn_xTe$ THIN FILMS

1. Growth of $Pb_{1-x}Sn_xTe$ Films

Seven different compositions of $Pb_{1-x}Sn_xTe$ were studied. The compositions studied are shown in Table 3-1. The films ranged from 0.8 to 5.0 microns in thickness and were grown on freshly cleaved (100) faces of KCl by a one-boat evaporation method [15]. In the one-boat evaporation, coarse particles of $Pb_{1-x}Sn_xTe$ were used as source material. Figure 3-1a shows the entire deposition system.

KCl substrates were used mainly because it has a cutoff wavelength of nearly 20 microns. The KCl substrate easily facilitated cross-secional cleaving on the film-substrate system for thickness determination on the scanning electron microscope.

2. Film Analysis

The crystalline structure of all $Pb_{1-x}Sn_xTe$ films were examined by the Laue x-ray back reflection technique. The x-ray analysis showed that all films were single crystal, indicated by the absence of Debye rings in the Laue pictures. See Figure 3-1b.

The orientation and lattice constant a for the films were determined from x-ray diffraction patterns obtained from a Norelco diffractometer using a copper target as the x-ray source. This information was then used to verify the composition of the films.

The carrier concentration of the optical samples was also obtained from electrical measurements taken on Hall samples deposited simultaneously with the optical samples. The concentration for the

TABLE 3 - 1

$Pb_{1-x}Sn_xTe$ OPTICAL SAMPLES STUDIED

SAMPLE NUMBER	X	SUBSTRATE
1	0.0	KCL
2	0.0	KCL
3	0.06	KCL
4	0.06	KCL
5	0.12	KCL
6	0.12	KCL
7	0.18	KCL
8	0.18	KCL
9	0.24	KCL
10	0.24	KCL
11	0.70	KCL
12	0.85	KCL

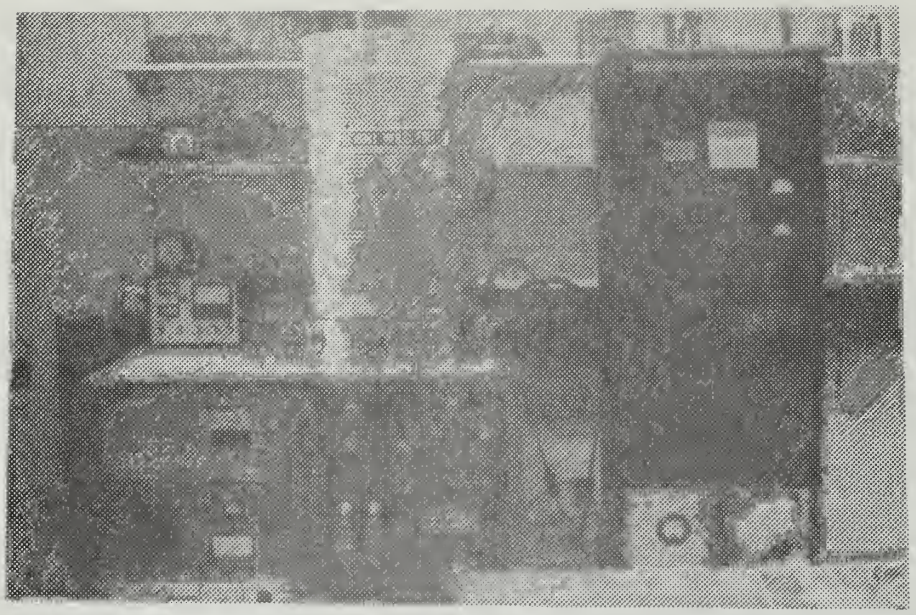

FIG. 3-1A - Deposition system used in making $Pb_{1-x}Sn_xTe$ optical samples.

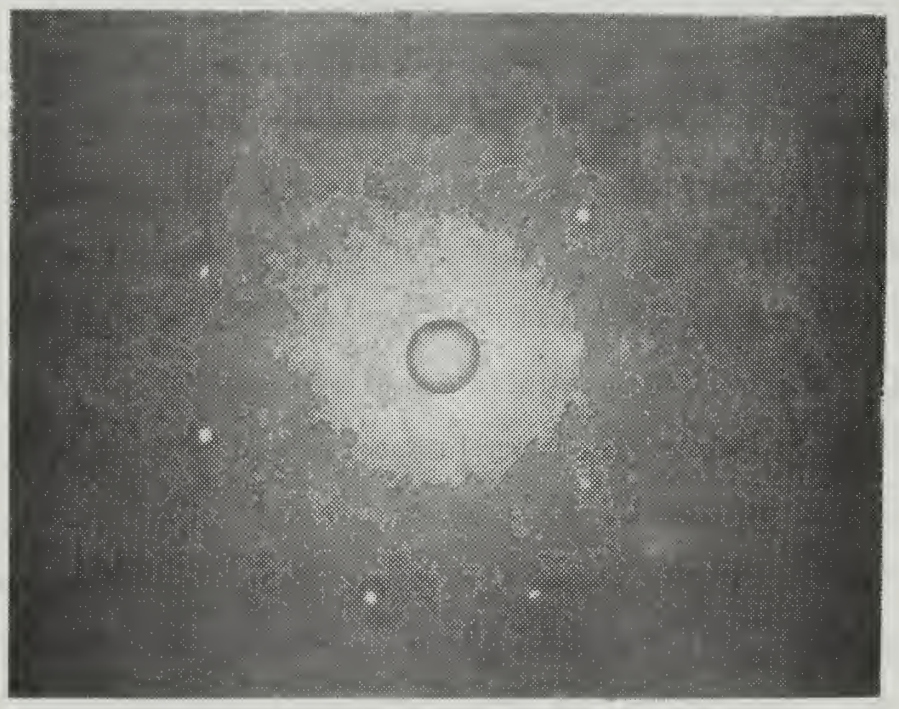

FIG. 3-1B - Laue picture of a $Pb_{1-x}Sn_xTe$ optical sample. The absence of faint Debye rings indicates single-crystalline growth.

p-type were in the range of low 10^{18} holes/cm^3 for $x \leq 0.24$ and low 10^{19} holes/cm^3 for $x = 0.70$ and $x - 0.85$.

Figure 3-2 shows a typically prepared $Pb_{1-x}Sn_xTe$ optical sample deposited on a KCl substrate. Typical films had an area of 1 cm^2. In general these films had a very uniform surface which required no further treatment following deposition to make then suitable for optical measurements. The films were shiny with clean flat surfaces. A few films showed minute clevage steps and pinholes.

B. REFLECTANCE AND TRANSMISSION MEASUREMENTS

1. Experimental Apparatus and Techniques

The optical measurements involving reflection and transmission were made in the 2.5 to 20 micron region using a Perkin-Elmer Model 621 recording double-beam spectrophotometer equipped with gratings, source, and thermocouple detector. A Beckman double-beam reflectance attachment was used in conjunction with the 621 for reflectance measurements.

Fow low temperature measurements the optical sample was mounted on a copper cold finger attached to a liquid nitrogen dewar capable of continuous temperature variation between room and liquid nitrogen temperatures. The dewar assembly was attached to an adjustable optical mount which enabled optimum optical alignment and rigidity in positioning the optical sample. Figure 3-3 shows the low-temperature experimental setup showing the spectrophotometer and low-temperature apparatus in the transmission mode. Figures 3-4a and 3-4b show the spectrophotometer and low-temperature apparatus in the reflection mode. The Beckman double-beam reflectance assembly is shown installed in the sample area.

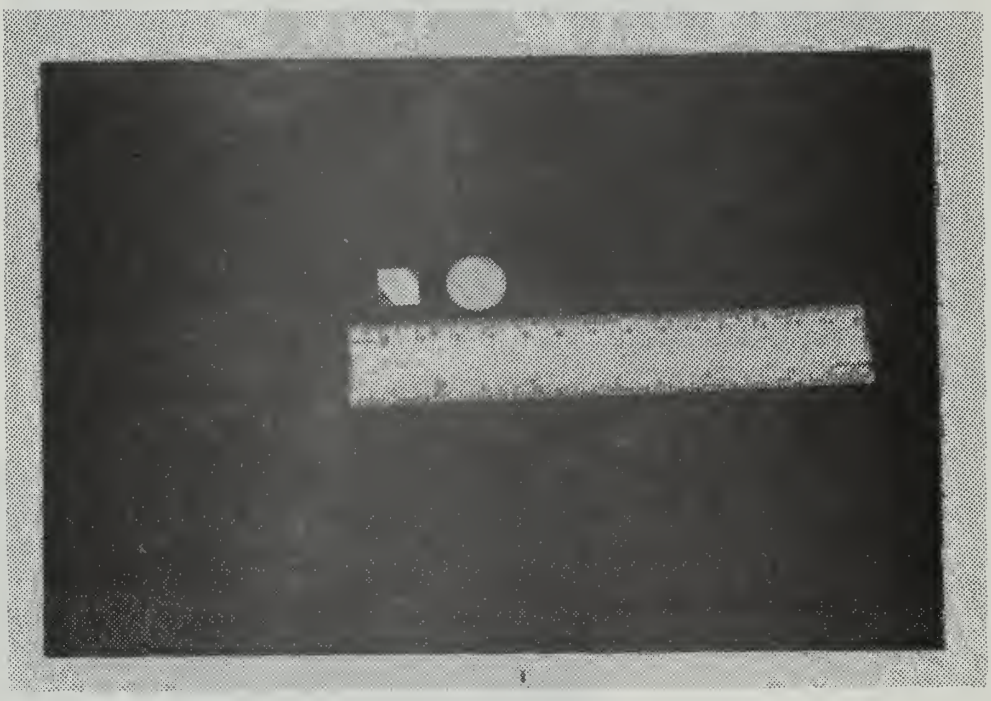

FIG. 3-2 - TYPICALLY PREPARED $Pb_{1-x}Sn_xTe$ FILM ON A KCL SUBSTRATE.

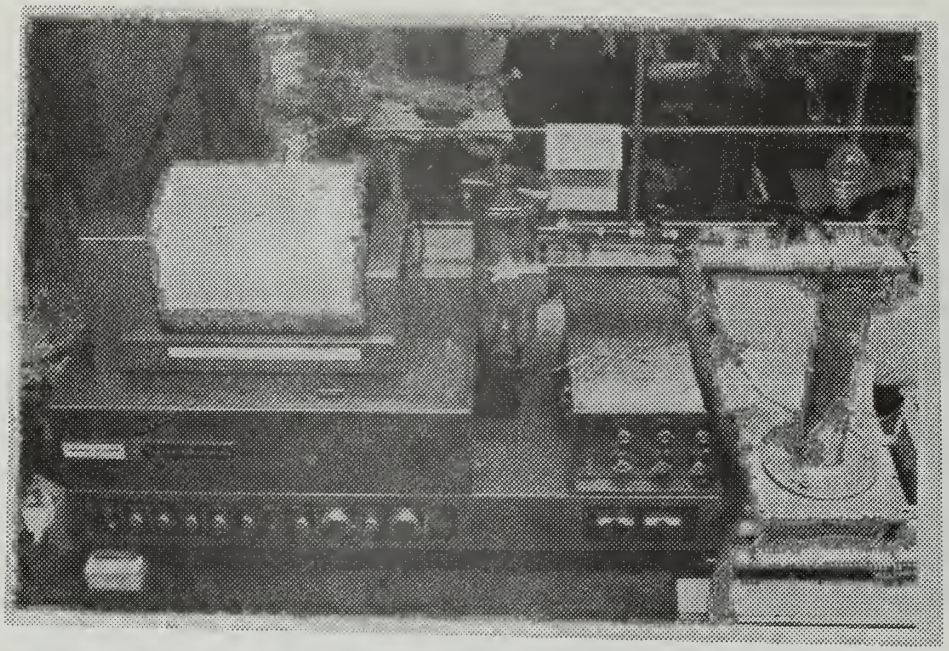

FIG. 3-3A - Spectrophotometer and low-temperature dewar in the transmission mode.

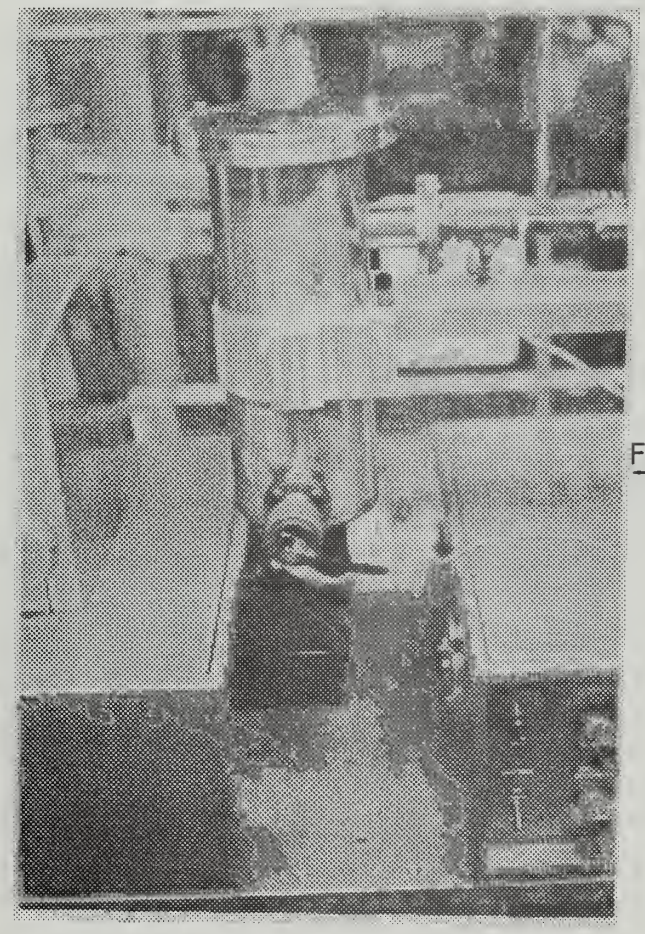

FIG. 3-3B - Low-temperature dewar assembly in sample beam.

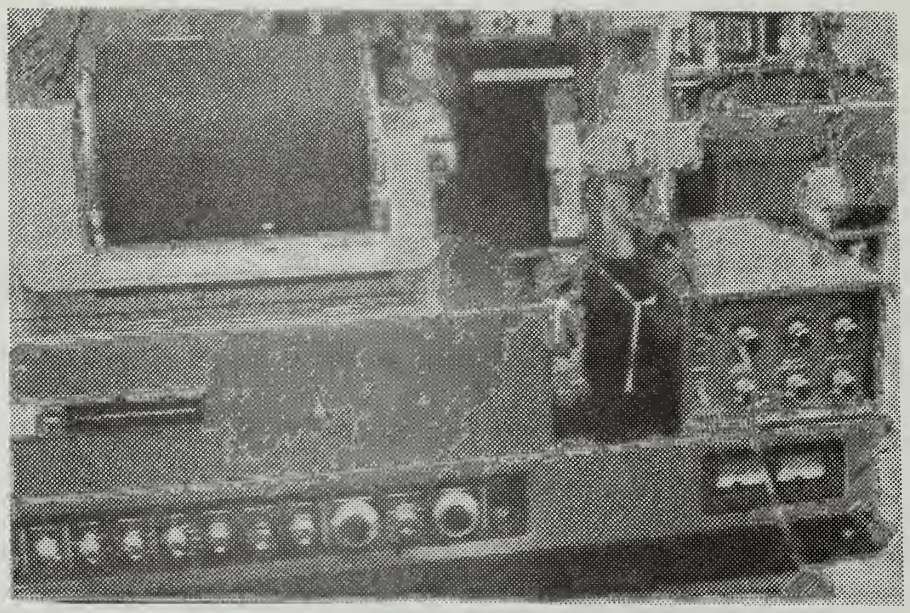

FIG. 3-4A - Low-temperature dewar assembly aligned for reflection measurements.

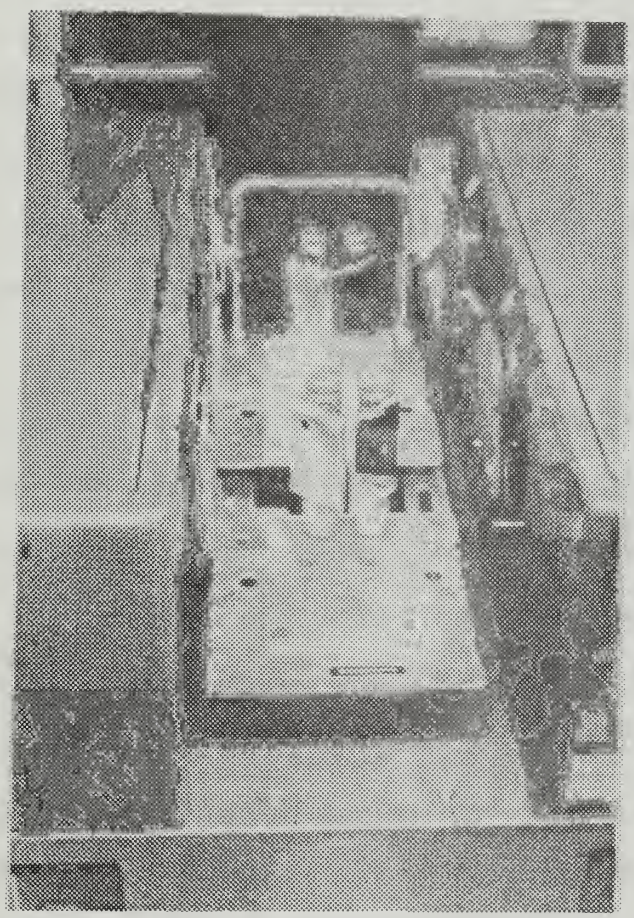

FIG. 3-4B - Beckman reflectance assembly installed in sample area.

A very important component of the spectrophotometer is the optical attenuator which is mounted in the path of the reference beam. The a.c. signal resulting from an unbalance in signal between the reference and sample beams activates a servo-mechanism which moves the optical attenuator, which is usually a wedge or comb that is mounted in the path of the reference beam. The comb is moved into the beam thus reducing the energy until both beams are balanced again. Figure 3-5 shows the schematic diagram for the transmission and reflection modes for the Perkin-Elmer 621 spectrophotometer.

The accuracy of the spectrophotometer is markedly degraded for low transmittance and reflectance values, typically below 10% where only the tip region of the optical attenuator comb is in the reference beam. Inaccuracies in the T and R data are introduced. Improved low transmission measurements were obtained by placing calibrated metal attenuating screens in the reference beam causing the optical attenuator to operate in its more linear or accurate region. This screen resulted in amplified transmission readings.

The accuracy of the transmittance and reflectance spectra traced on the chart paper depended on the speed and sensitivity of the detector and amplifier. For this study a scan from 2.5 to 20 microns took 25 minutes which assured good accuracy and resolution.

A schematic of the low-temperature apparatus is given in Figure 3-6. The optical sample was held rigidly by the use of spring-loaded pressure contacts which held the sample securely to the copper cold finger. The use of spring-loaded clips permitted optimum positioning of the thin film-substrate system and at the same time there was no damage to the film. The vacuum enclosure around the cold finger

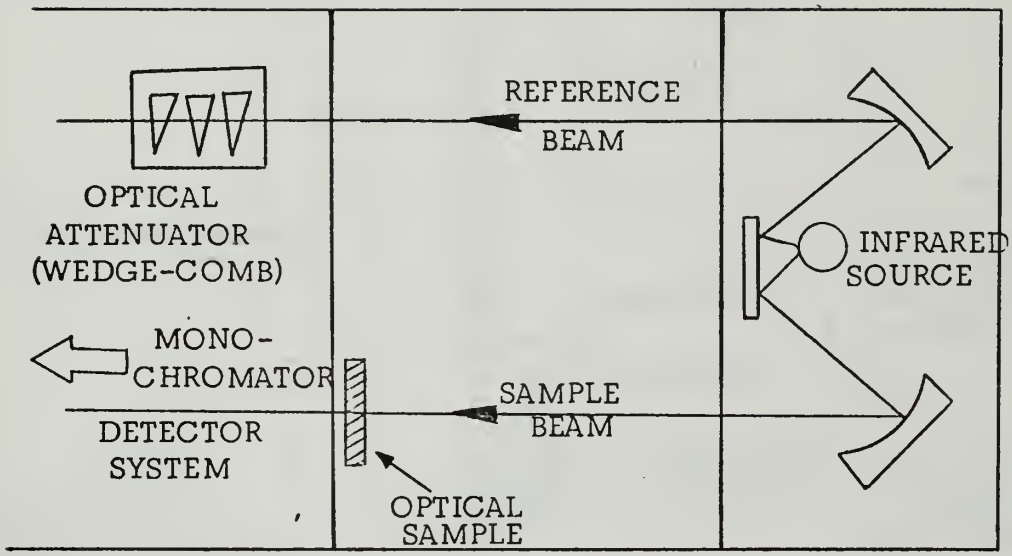

(a) TRANSMISSION MODE

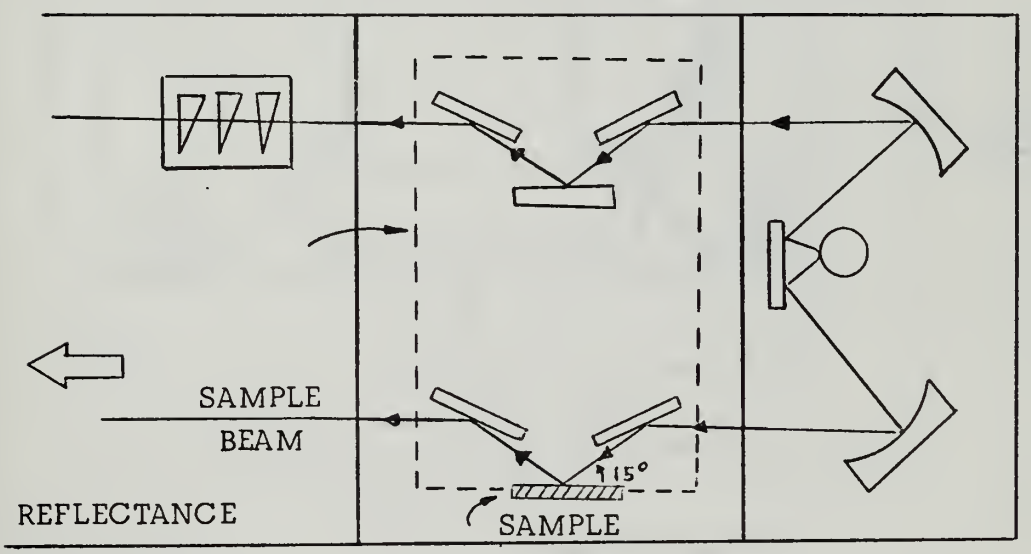

(b) REFLECTION MODE

Figure 3-5

Schematic Diagrams of the Transmission and Reflection Modes for the Spectrophotometer.

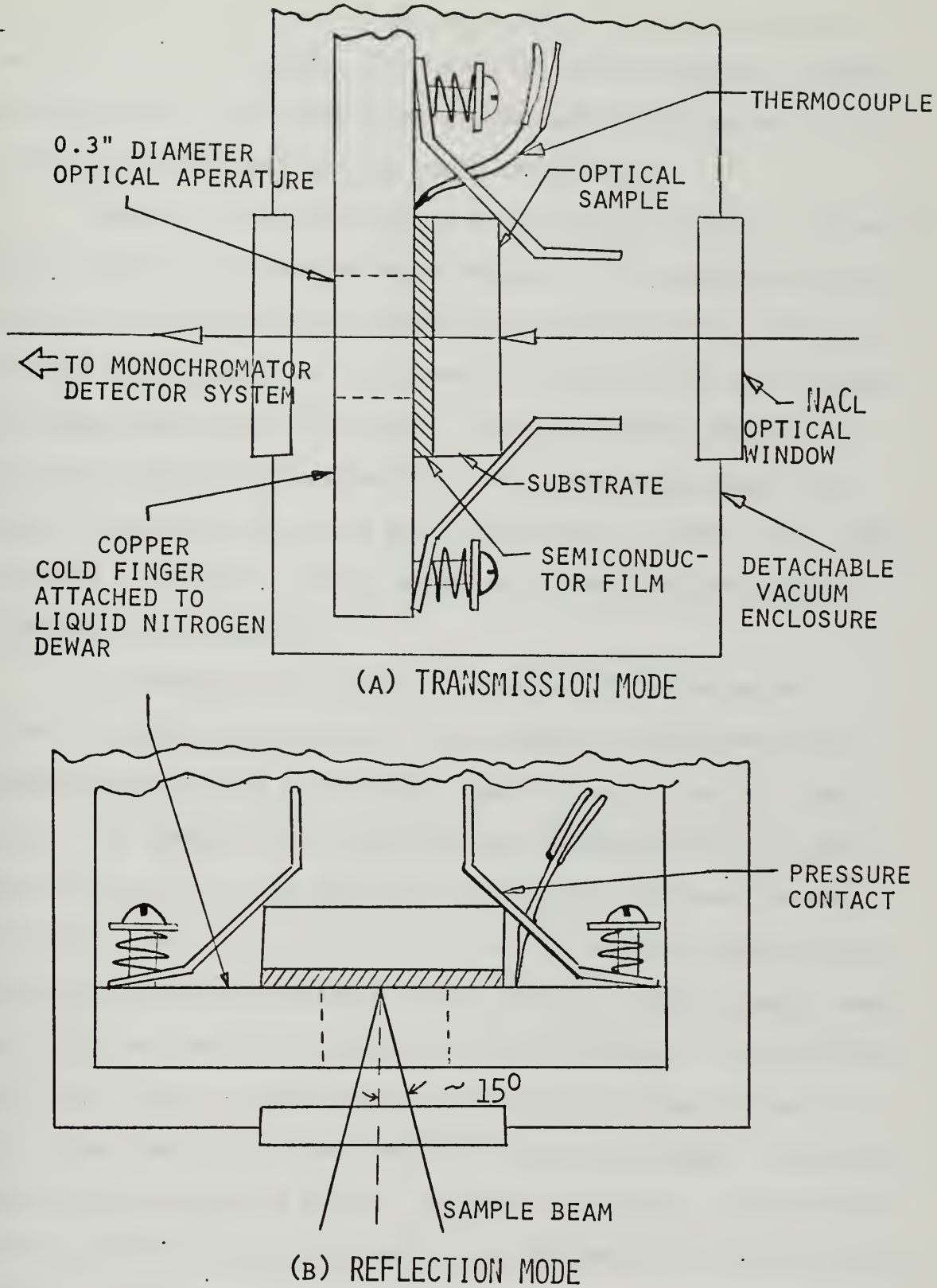

FIG. 3-6 - SCHEMATIC DIAGRAMS OF LOW-TEMPERATURE MEASUREMENT TECHNIQUES.

was held in place by virtue of the vacuum only. This permitted easy changing of optical samples. The vacuum was needed to maintain thermal isolation of the cooper cold finger at low temperatures and to prevent condensation of atmospheric water vapor on the sample.

Figure 3-7 shows the position of the vacuum enclosure. The optical windows used in the vacuum enclosure were NaCl. This material was chosen because of its relatively high transmittance of 0.92 out to 16 microns. Its chief disadvantage was its hygroscopic nature but this was overcome by frequent polishing of the window. Since the film was deposited on KCl which transmits out to 20 microns, the optical measurements were actually filtered by the use of NaCl as the optical windows. KCl windows would have overcome this limitation but were unavailble when these measurements were conducted.

In performing the "sample-in", "sample-out" technique the following procedure was followed. For transmission measurements the reference material used in the sample beam only was a blank KCl substrate. The "sample-out" transmission spectra obtained with only the substrate material in the sample beam yielded the 100% transmittance calibration line. This 100% transmittance line was also taken as 100% calibration for all low-temperature measurements. Next the sample beam was blocked and the 0% transmittance line was obtained. The 100% and 0% calibration lines were both taken with the optical vacuum enclosure in place. Next the transmission "sample-in" mode was performed. The blank substrate was replaced by the $Pb_{1-x}Sn_xTe$ optical sample. The room temperature (300°K) transmittance spectra was obtained first. Next arbitrary temperatures between room and liquid nitrogen temperatures were obtained by cooling the cold finger with liquid nitrogen. In this study transmission spectra were obtained for temperatures of 300°K, 195°K, and 80°K.

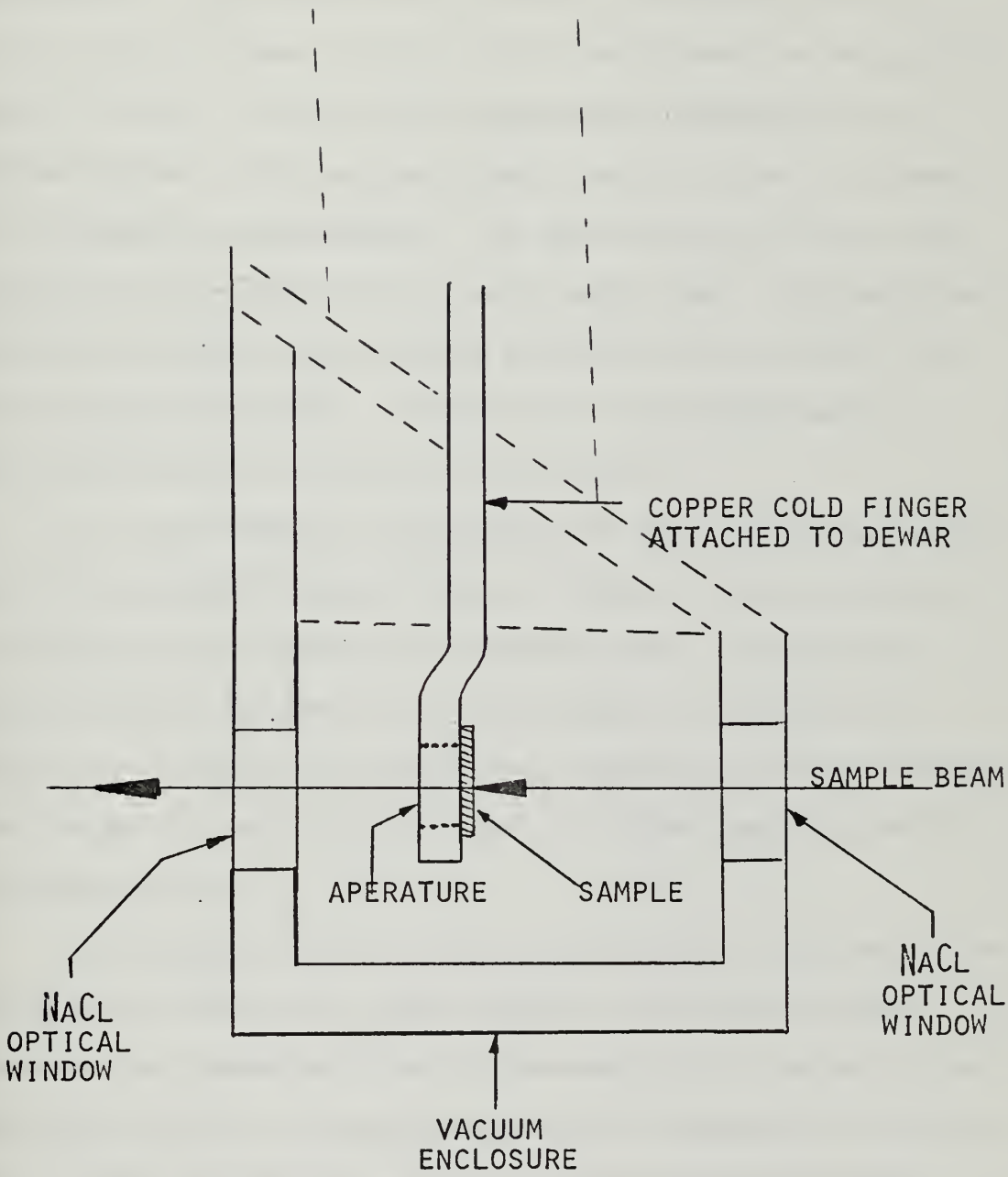

FIG. 3-7 - CROSS-SECTION OF COLD FINGER AND SAMPLE AREA INSIDE VACUUM ENCLOSURE.

The reflection spectra were obtained using a slightly different procedure. The reference material used was aluminum evaporated on polished glass. The reflectance of similarly prepared aluminum is given as varying between 0.97 and 0.99 in the infrared for temperatures down to 77°K [16]. Thus, the room temperature reflectance of the aluminum scanned on the spectrophotometer was also taken as reference for low-temperature measurements. The 100% reflection line was thus obtained with the aluminum mirror in the sample beam. The sample position was left empty to obtain the 0% calibration line. Finally the optical sample was scanned. All reflection measurements were also taken with the optical enclosure vacuum mounted.

For low transmission measurements the metal attenuating screens with calibrated magnification factors of 3.05X and 8.75X were used in the reference beam to amplify the recording levels. The apparent sample reflection and transmission recordings obtained using the "sample-out", "sample-in" procedure were adjusted with the calibration lines and amplification factors to obtain the true sample reflectance R and transmittance T.

The $Pb_{1-x}S_nTe$ film was held in direct contact with the polished surface of the copper cold finger by means of the pressure contact. A copper-constant thermocouple was pressure-mounted onto the cold finger adjacent to the film. It was assumed that the thermocouple monitoring the cold finger temperature would also yield the film temperature. Initial measurements showed that the cold finger reached 80°K when the cold finger was in thermal equilibrium with the dewar filled with liquid nitrogen which has a temperature of 77°K. Temperature measurements taken with the thermocouple mounted on the substrate side of

the film-substrate system showed a 5°K difference than the cold finger. This seems to indicate the proximity of the film temperature to the cold finger temperature.

The easy "sample-in", "sample-out" procedure owing to the vacuum held sample enclosure and the pressure-mounted sample yielded important implications in terms of the experimental results. The rigid mounting of the dewar system eliminated the possibility of disturbing the optical alignment of the sample mount and minimized any changes in the optical signal path when the experimental procedure was carried out. These considerations were very important in the reflection measurements because of the critical sensitivity in the adjustment of the reflectance assembly. A small change in the sample alignment introduced a substantial error in the reflection measurement.

It was attempted to perform the separate transmission and reflectance measurements on the middle section of the optical sample. Use of identical circular apertures with relatively large areas for the sample mount (0.6 cm^2) and approximately 1 cm^2 for the films minimized the mismatch of the film region.

The cold finger was cooled by adding minute quantities of liquid nitrogen into the dewar. Stable temperatures throughout the temperature range between 80°K and 300°K were easily maintained for periods in which the spectrophotometer scans were taken place. This was made possible by the large copper block situated at the bottom of the liquid nitrogen chamber in the dewar to which the cold finger was attached. This system behaved as a stable thermal resevoir.

A scanning rate of 25 minutes for the entire wavelength range from 2.5 to 20 microns was used. This scanning rate was found to be

a good compromise because it was sufficiently slow to show any fine structure but at the same time short enough so that stable low temperatures could be maintained.

Room temperature reflectance and transmittance measurements were obtained with and without the low-temperature optical enclosures. Many of the low temperature scans were also checked for reproducibility.

2. Experimental Results

A typical transmission and reflection recording from the Perkin-Elmer 621 spectrophotometer is shown in Figure 3-8. The 100% reference calibration line shows variations owing to the inherent behavior of the spectrophotometer as well as effects of atmospheric absorption. Large jumps were caused by grating changes. For transmission levels below 10%, amplified recordings were made using the calibrated metal screens. In determining the actual reflectance and transmittance readings the behavior of the calibration lines were proportionally accounted for.

C. DETERMINATION OF FILM THICKNESS

Accurate thickness determination is a prerequisite in using the interference fringe method (Eq. 2-26) to determine the index of refraction. The thickness d is also required in evaluating the R-T equations for the absorption coefficient. The accuracy of d is less stringent in this case.

There are a number of film thickness measurement methods. Some methods can be used only at the film edges which are away from the region in which most of the optical measurements were made. Some methods require the index of refraction itself. In this study the scanning electron microscope was used to determine film thickness.

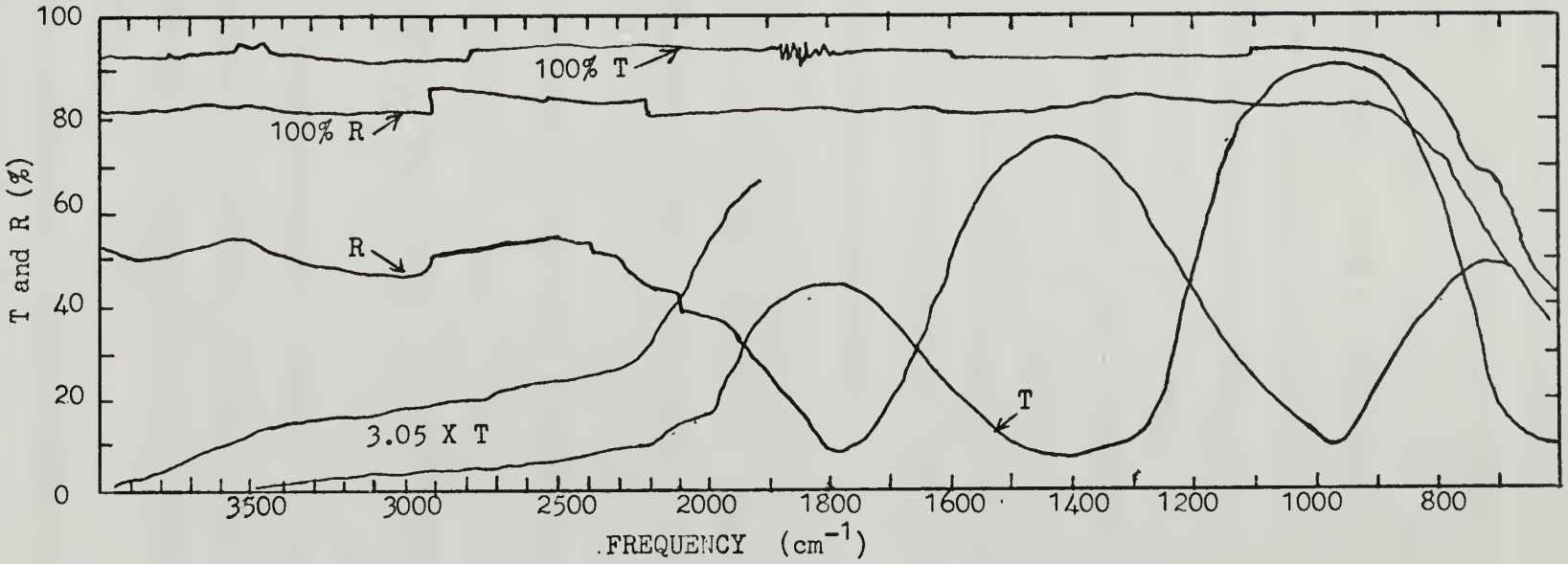

FIG. 3-8 - TYPICAL SPECTROPHOTOMETER RECORDING OF REFLECTION AND TRANSMISSION MEASUREMENTS ($Pb_{0.94}Sn_{0.06}Te$; d = 0.85μ)

After all the optical transmission and reflection measurements were completed, the thickness of the optical samples were measured. By cleaving the semiconductor cross-sectionally and magnifying it, the thickness can be determined, knowing the magnification factor. Owing to the orthogonal cleavage planes of the KCl substrate, the $Pb_{1-x}Sn_xTe$ films were found to cleave in the same manner when cleaved from the substrate side. The optical samples were cleaved across the film region where the optical measurements had been made. Then the film-substrate cross-section was coated with gold. The scanning electron beam was then focused on the cross-section revealing a bright region which corresponded to the highly reflected beam from the semiconductor film. The gold coating prevented the dielectric substrate from accumulating electrons and showing bright areas.

The scanning electron microscope measurements were conducted by the Applied Space Products of Palo Alto, California. Measurements were made at 10K and 20K magnification. A calibration grid (no. 1749, standard for ESM, Ernest F. Fullman, Inc.) having 2160 lines/mm was used. Scans of the calibration grid were made at 20K and 10K. The calibration grid was aligned to yield one set of parallel ruled lines normal to the electron beam and hence maximum separation distance. The calibration was claimed to be accurate to 0.02 micron. Figure 3-9 shows the calibration grid at 20K magnification. Figure 3-10 gives a typical representation of a thin film cross-section observed with the scanning electron microscope. The rough irregular features of the film cross-section were probably due to cleaving.

The film thickness was determined at several regions across the film cross-section where the optical measurements were made. An average

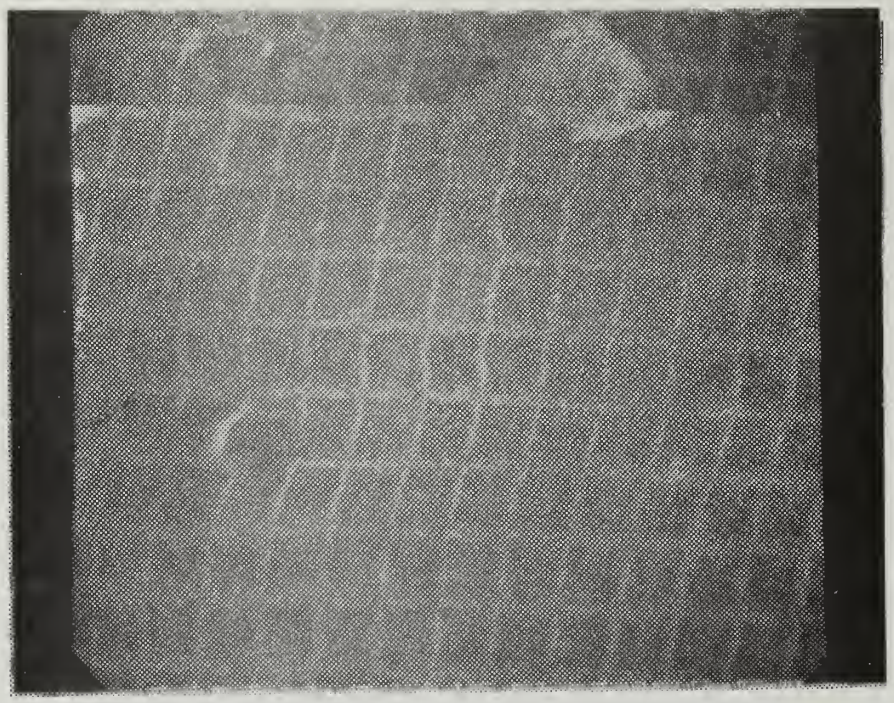

FIG. 3-9 - CALIBRATION GRID FOR ELECTRON SCANNING MICROSCOPE AT 20K MAGNIFICATION.

FIG. 3-10 - PBTE SAMPLE CROSS-SECTION AT 10K MAGNIFICATION.

value for d was obtained from these measurements. The film thickness varied typically 5% or less in this region. Table 3-2 gives the results of the film thickness measurements for the $Pb_{1-x}Sn_xTe$ samples evaluated in this study.

TABLE 3 - 2

RESULTS OF THICKNESS MEASUREMENTS ON $Pb_{1-x}Sn_xTe$ OPTICAL SAMPLES

SAMPLE NUMBER	X	THICKNESS(μ)
1	0.0	-
2	0.0	2.63
3	0.06	4.90
4	0.06	0.85
5	0.12	5.25
6	0.12	2.70
7	0.18	4.98
8	0.18	1.77
9	0.24	4.86
10	0.24	1.54
11	0.70	1.27
12	0.85	1.60

IV. RESULTS AND DISCUSSION

A. REFLECTANCE AND TRANSMITTANCE SPECTRA

The actual transmittance and reflectance spectra were obtained for the $Pb_{1-x}Sn_xTe$ films by adjusting the experimentally obtained T and R data from the spectrophotometer scans with the 100% and 0% calibration lines. The error in R and T is estimated to be ± 6%, except for low transmission values (≤15%), in which T is estimated to be within 10%. Typical reflectance and transmittance spectra for various temperatures and compositions are given by Figures 4-1. They include x = 0.06, 0.24, and 0.70. The behavior of the transmittance and reflectance spectra in the infrared for the $Pb_{1-x}Sn_xTe$ films is characterized by the effects of film thickness, energy gap, and the number of bound and free carriers.

Thicker films displayed a higher frequence of interference fringe extrema in the spectral region where they are essentially transparent to radiation. This is described by Equation (2-26). The mismatch of the corresponding R and T spectra was also minimal in the region of the film transparency as indicated by the relative position of the maxima and minima. The regularity of the uniformly shaped fringes shown in Figures 4-1 as well as in all R and T spectra, suggests the uniformity of the film thickness in the region where the optical measurements were made.

The reflectance spectra is characterized by the effects of bound and free carriers. In the short wavelength region, below the onset of transmission, the incident optical frequencies are absorbed not only by loose bound carriers which subsequently make band gap transitions, but also by tighter bound carriers which cannot make band gap transitions.

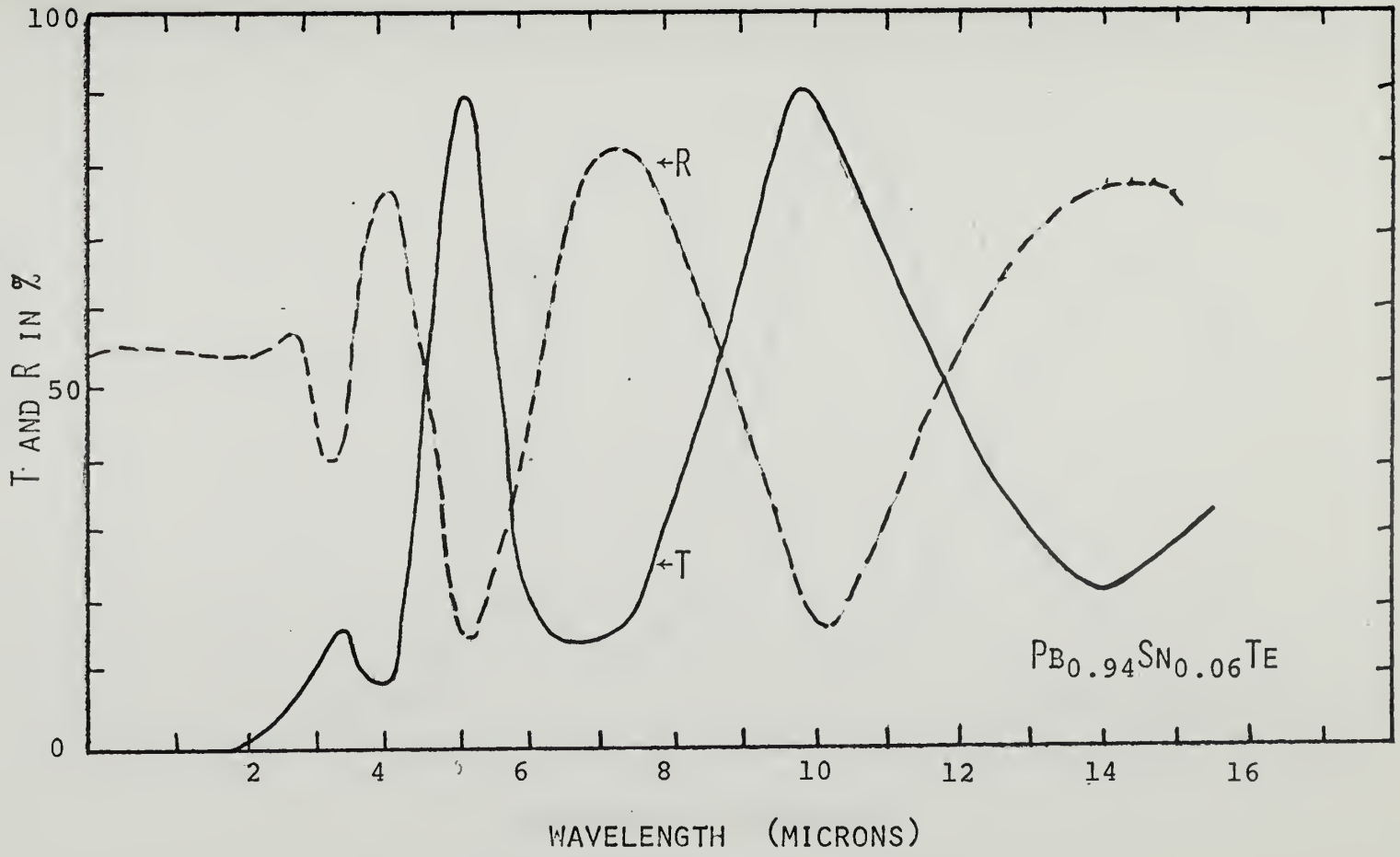

FIG. 4-1 -- TYPICAL THIN FILM REFLECTANCE AND TRANSMITTANCE SPECTRA FOR $Pb_{1-x}Sn_xTe$.

FIGURE 4-1A - $Pb_{0.94}Sn_{0.06}Te$; T = 300°K; D = 0.85μ

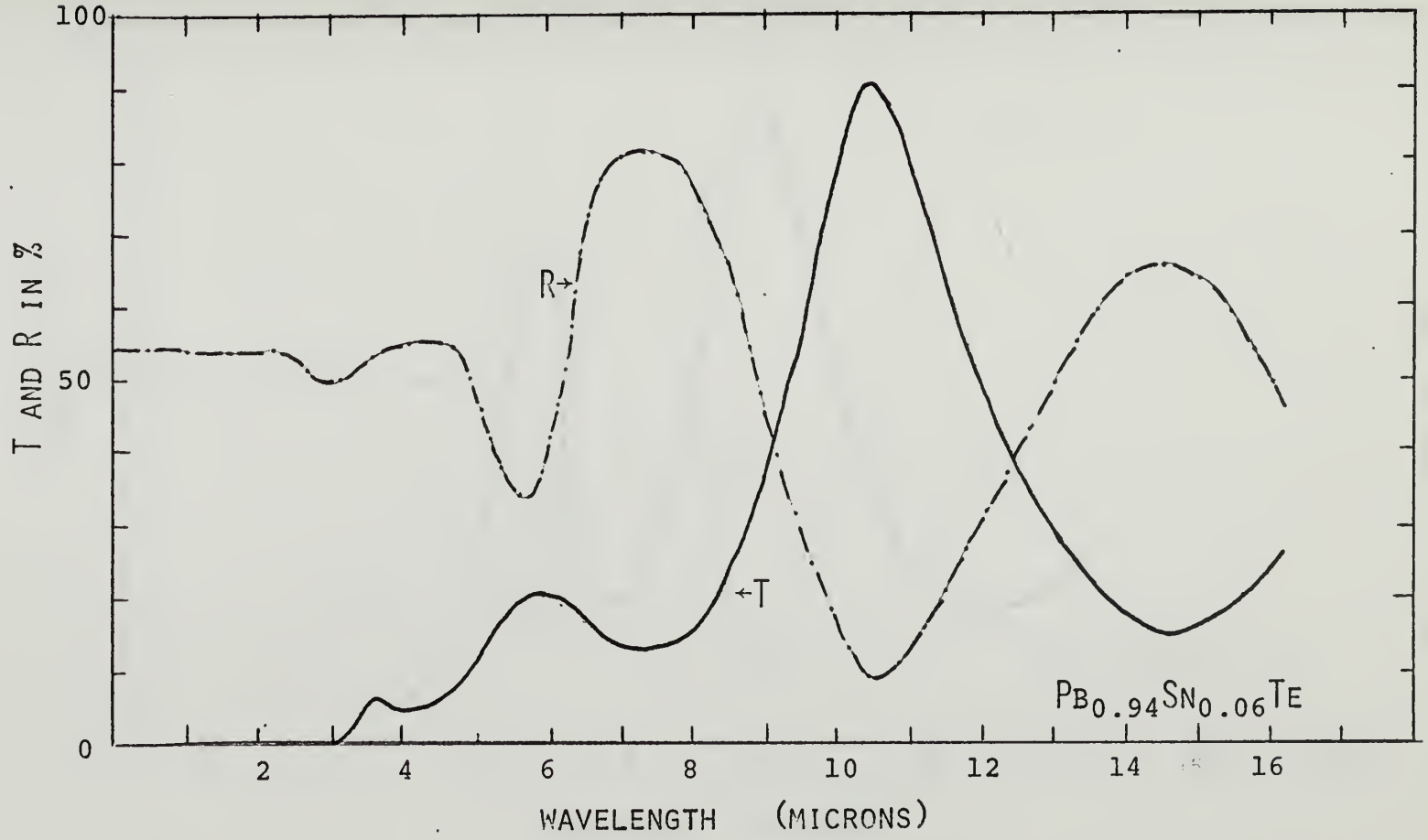

FIGURE 4-1B - $PB_{.94}SN_{0.06}TE$; T = 80°K; D = 0.85 μ

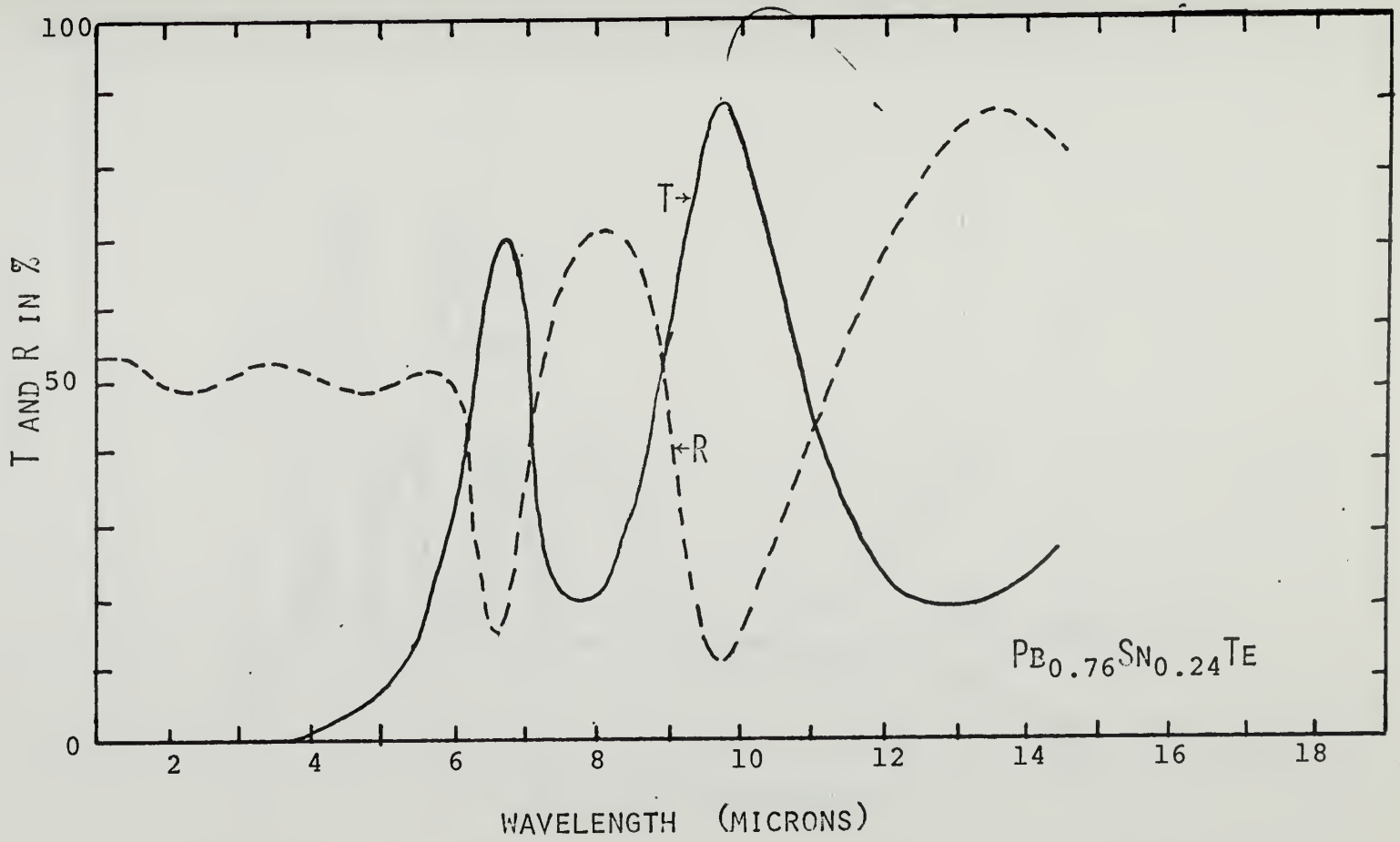

FIGURE 4-1c - $PB_{0.76}SN_{0.24}TE$; T = 300°K; D = 1.54μ

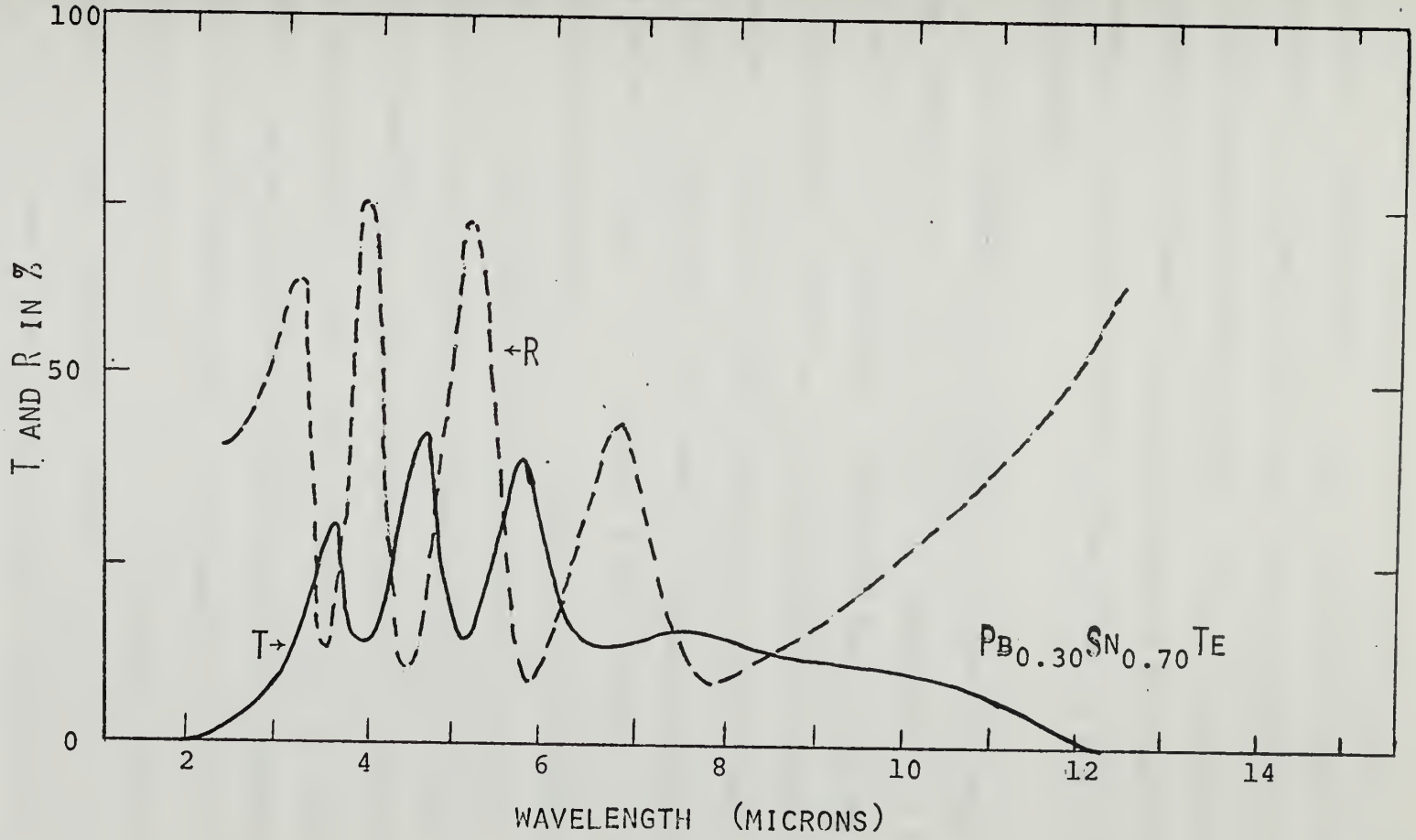

FIGURE 4-1D - $Pb_{0.30}Sn_{0.70}Te$; T = 80°K; D = 1.27μ

A slight amount of absorption in this frequency range is caused by free carriers. The absorption by tighter bound carriers and free carriers give rise to reflection which can be seen as essentilaly constant reflectance levels in the R spectra. Thus, in this spectral region the absorption of incident radiation resulting in band gap transition and bound and free carrier reflection accounts for the effectively zero transmittance.

It was attempted in this research to confirm the property of energy band inversion in $Pb_{1-x}Sn_xTe$ films. For compositions $x \leq 0.24$ the increase in film transmittance, related to energy band gap transitions by bound carriers, shifts to longer wavelengths or smaller photon energies as the film is cooled from room to liquid nitrogen temperatures. In terms of composition x, the onset of transmission was found to shift to longer wavelengths for $x \leq 0.24$ as x was increased. In order to confirm the band inversion for $Pb_{1-x}Sn_xTe$ [3] compositions of $x = 0.70$ and $x = 0.85$ should have exhibited an inverse shift. For $x \geq 0.50$ the energy gap should increase with decreasing temperature and x. Experimental transmittance curves showed no shift for $x = 0.70$ and 0.85 as the temperature was varied. This can be attributed to high free-carrier absorption owing directly to the high free-carrier concentration of these particular optical samples. This behavior is similar to that observed for SnTe films [14, 17]. The free carrier effect was more prominent at higher temperatures for these compositions since presumably the onset of transmission shifted to longer wavelengths for increased temperatures. This is seen by observing the increase of transmittance for lower temperatures in Figure 4-1. The compositions with $x \leq 0.24$ did not display free-carrier absorption behavior since the carrier

concentration of these samples was in the order of $10^{17} cm^{-3}$. The samples having x = 0.70 and 0.85 had free carrier concentrations in the high 10^{18} cm^{-3}. The effect of the increased number of free carriers was to essentially mask any evidence of band inversion which could have been observed using optical absorption methods.

B. OPTICAL CONSTANTS

1. The Index of Refraction

The index of refraction for thin $Pb_{1-x}Sn_xTe$ films was obtained using the interference fringe method. In determining the fringe order m by use of Equation (2-32), a rough estimate of the magnitude and wavelength dependence of the refractive index n was made. In general, the fringe order was determined without difficulty. The assignment of (m+1) and (m-1) instead of the true value of m produced unreasonable values of the calculated n.

For each composition of $Pb_{1-x}Sn_xTe$ studied, two films of different thickness were used to provide overlapping data. The index of refraction spectra for all compositions and temperatures are given by Figures 4-2. The uncertainty in the absolute values of n is estimated to be less than 4% owing essentially to the uncertainty in the film thickness. The relative error in the n values is probably much less owing to the high certainty in the wavelength positions of reflectance interference fringe extrema. Compositions with $x \leq 0.24$ had refractive index spectra which exhibited peaks which increased and shifted to lower photon energies with decreasing temperature. Although this dispersion of the refractive index is relatively small, it has an important effect on the absorption edge of $Pb_{1-x}Sn_xTe$. The refractive index peak actually corresponds to the position of the absorption edge or energy

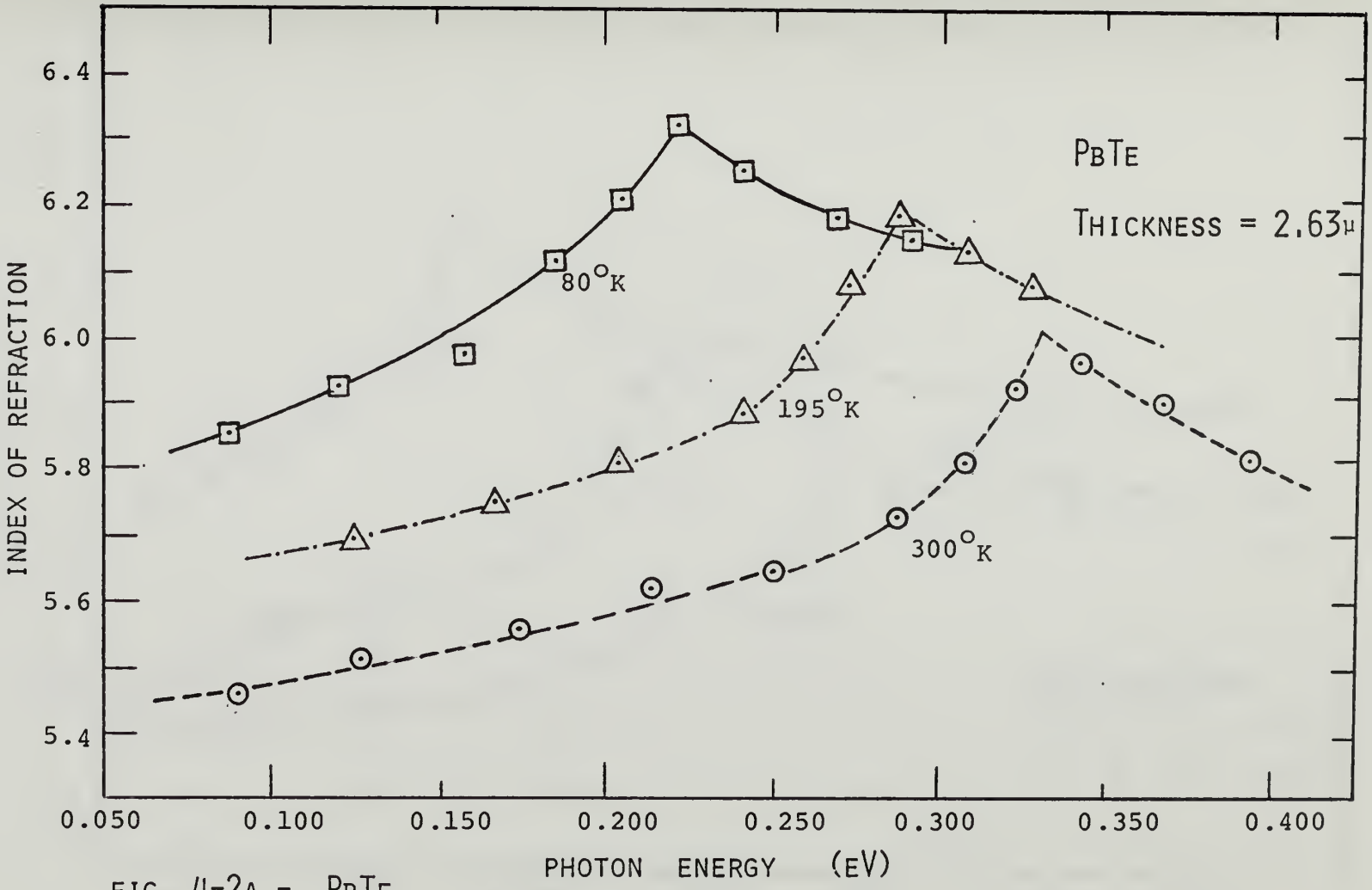

FIG. 4-2A - PBTE

Figure 4-2 Index of Refraction Spectra of Single-Crystal $Pb_{1-x}Sn_xTe$ Films.

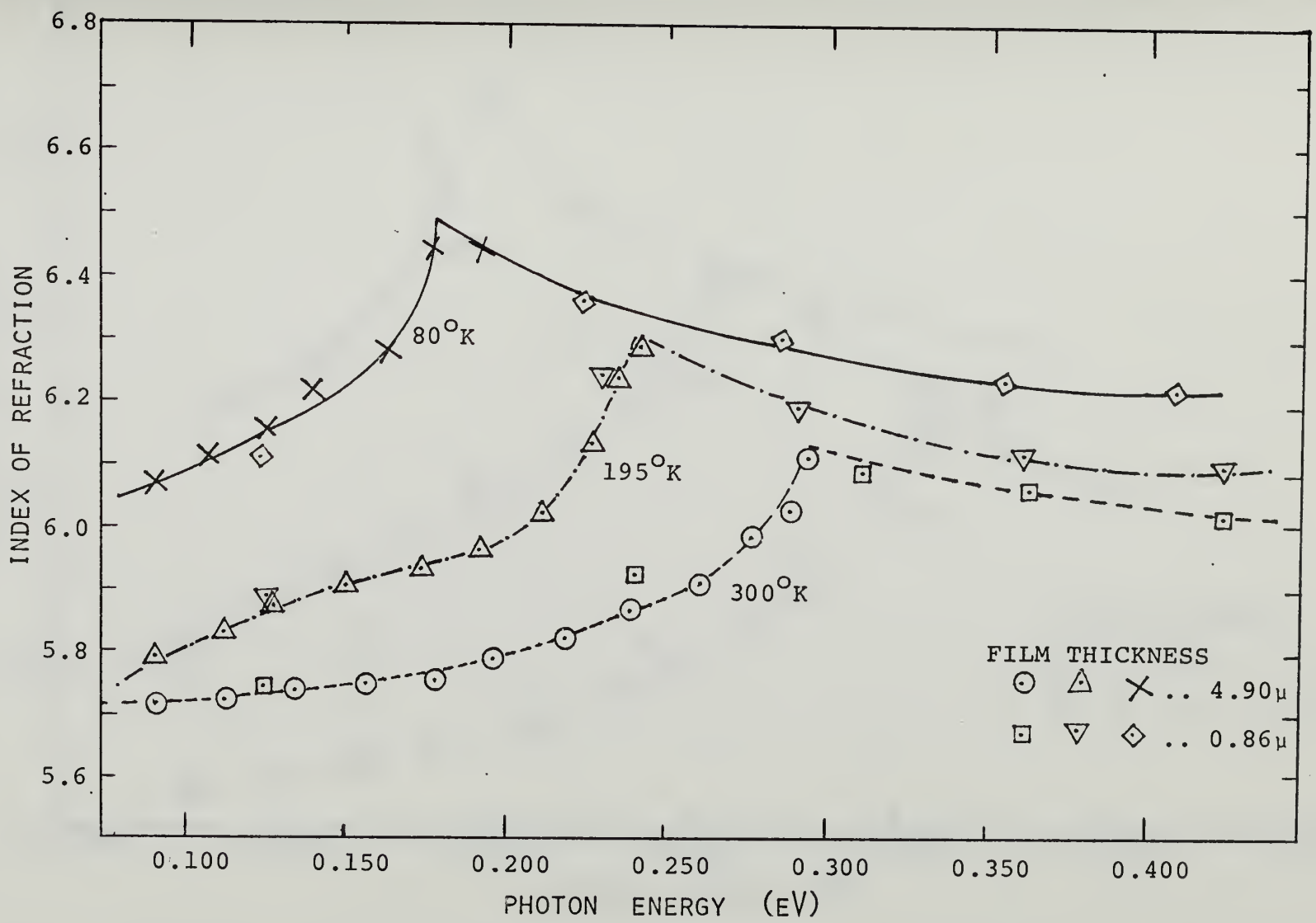

FIG. 4-2B - $Pb_{0.94}Sn_{0.06}Te$

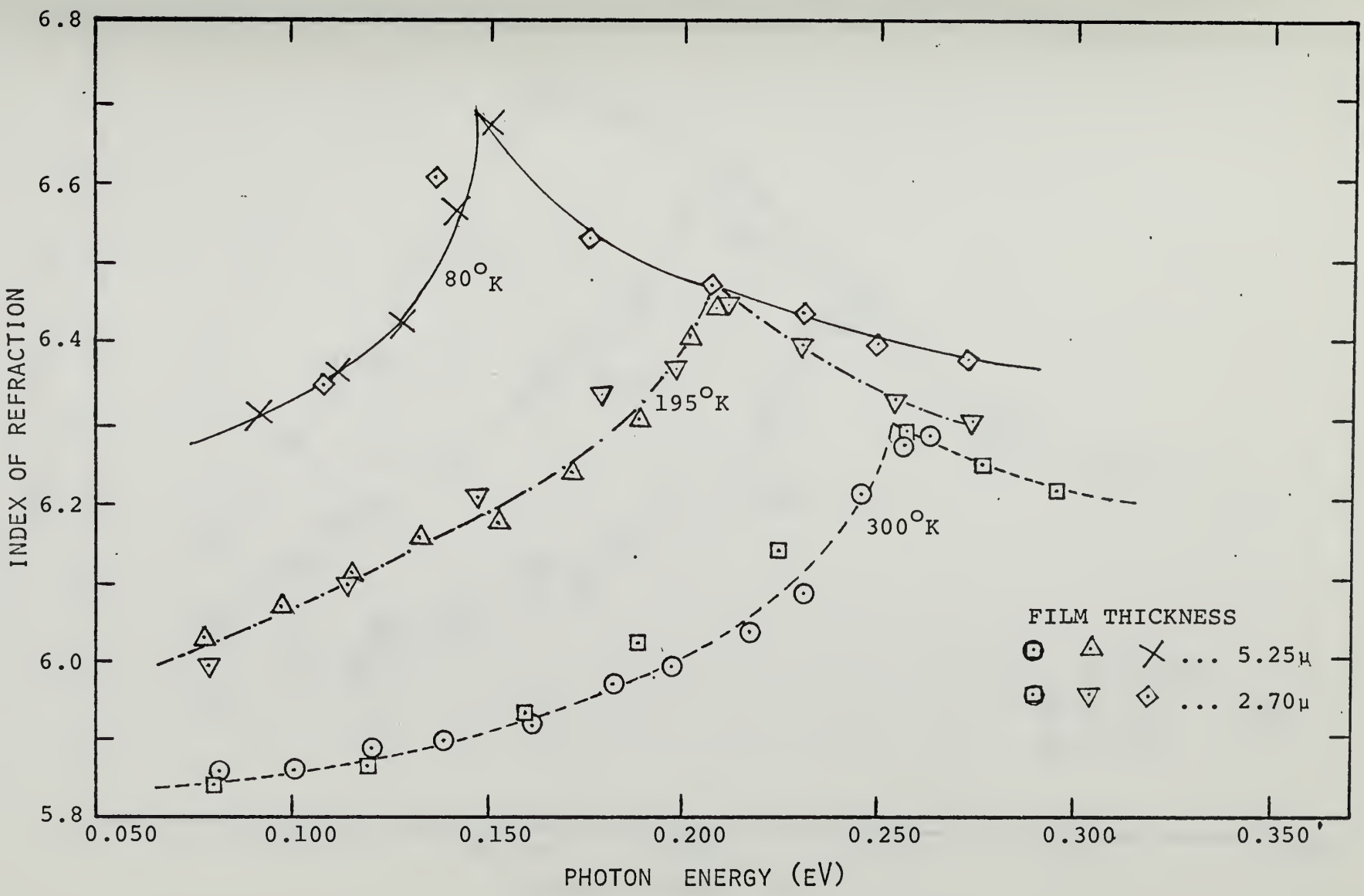

FIG. 4-2c - $PB_{0.88}SN_{0.12}TE$

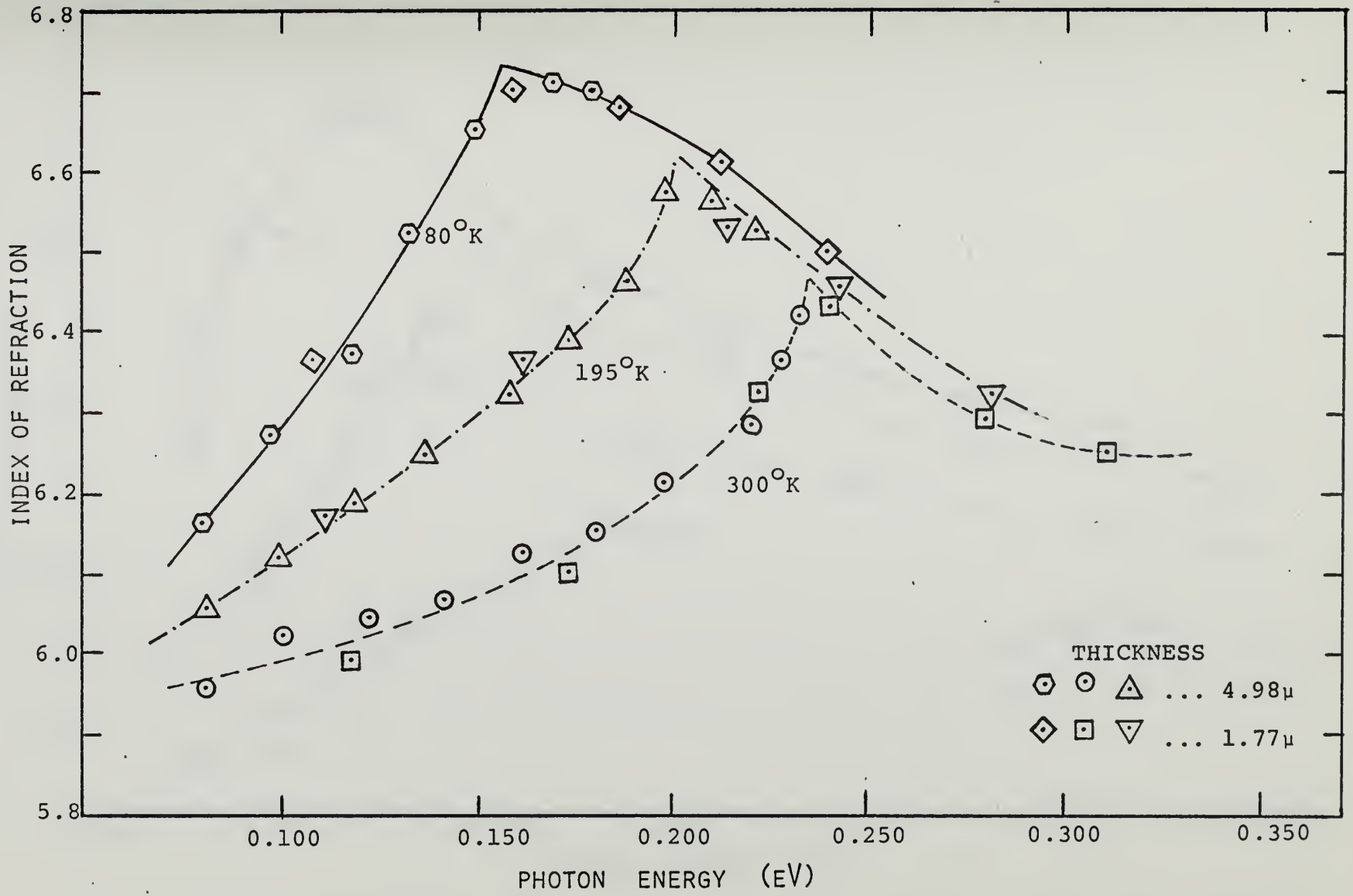

FIG. 4-20 - $Pb_{0.82}Sn_{0.18}Te$

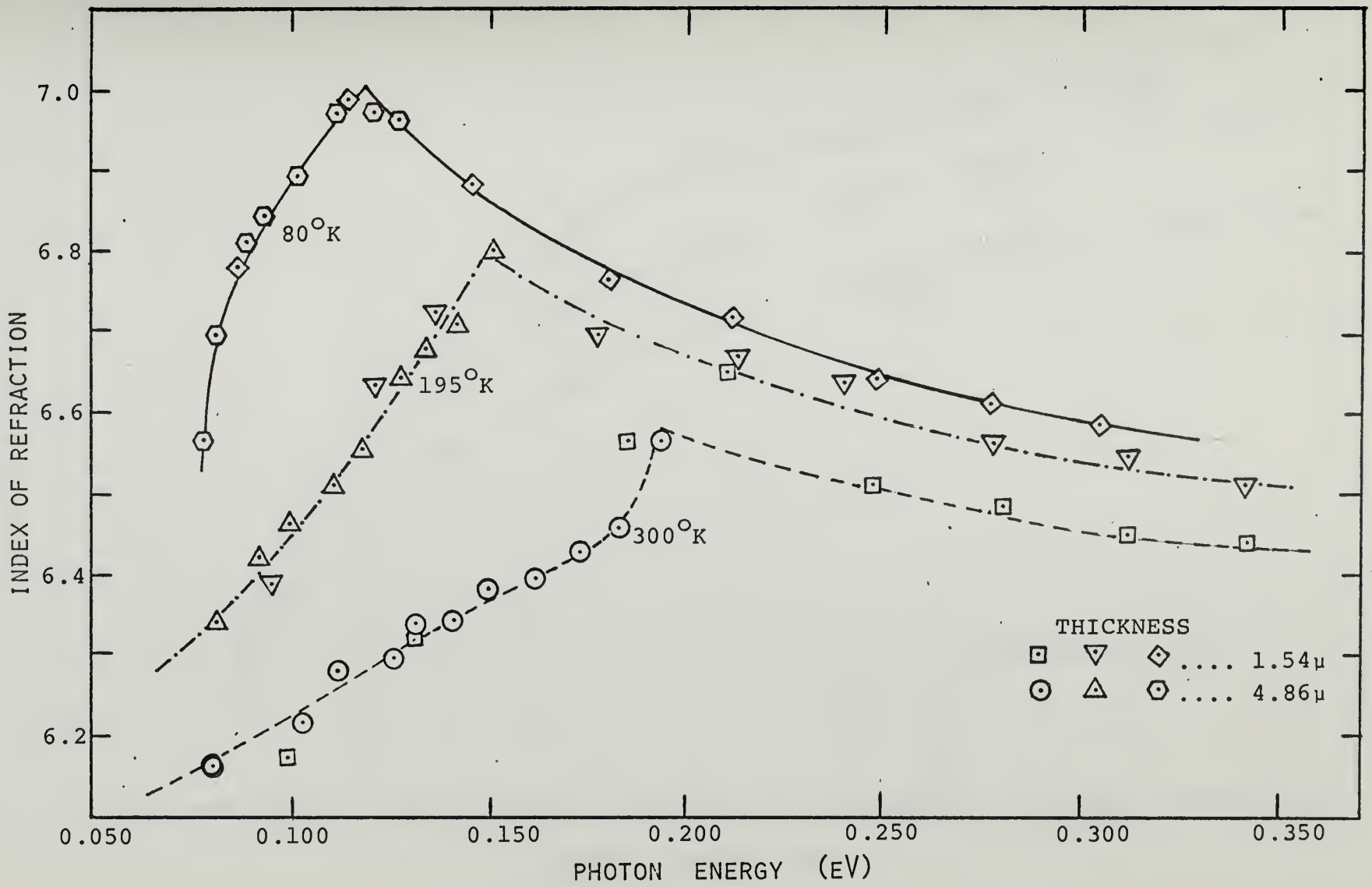

FIG. 4-2E - $Pb_{0.76}Sn_{0.24}Te$

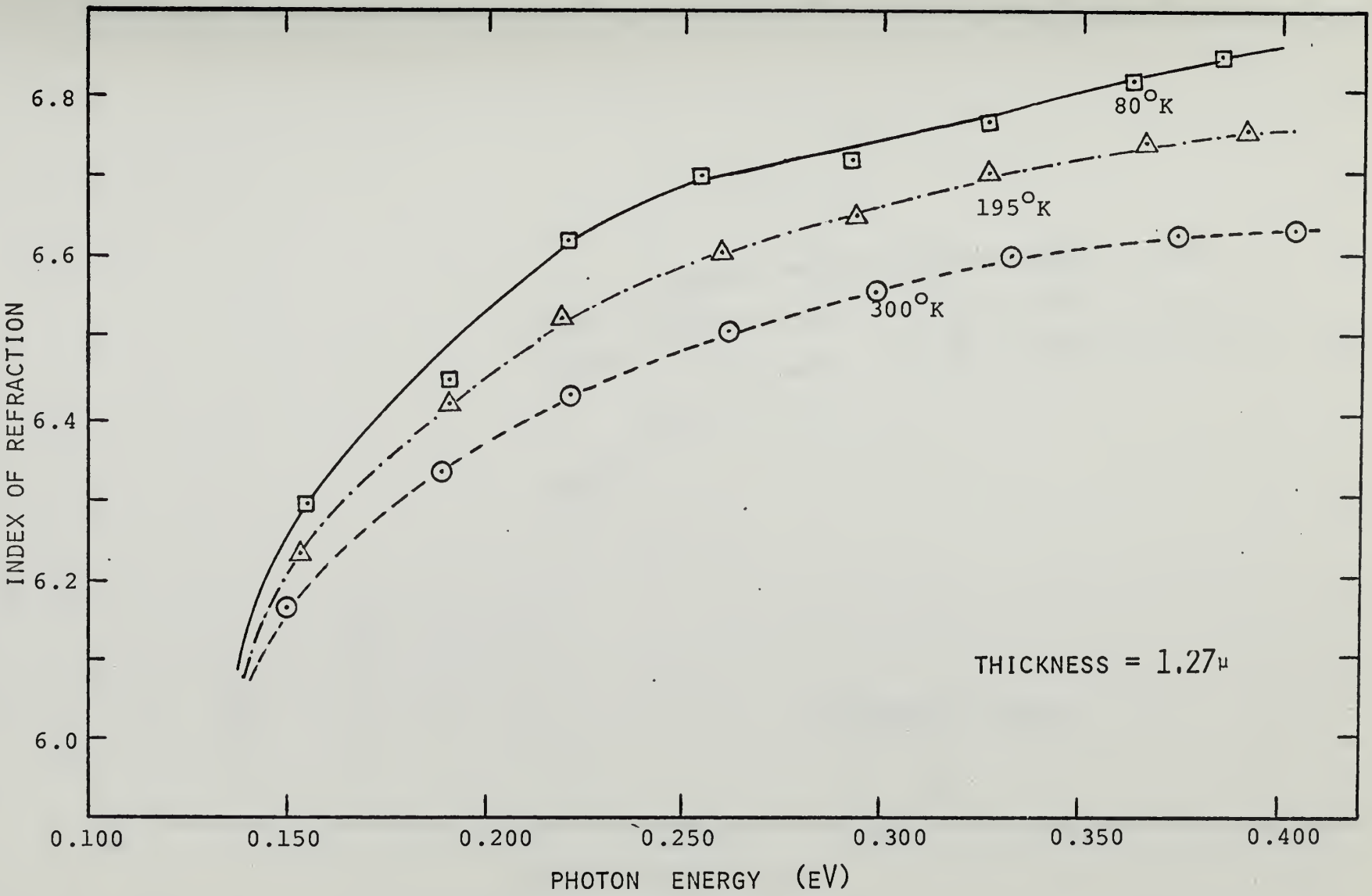

FIG. 4-2F - $PB_{0.30}SN_{0.70}TE$

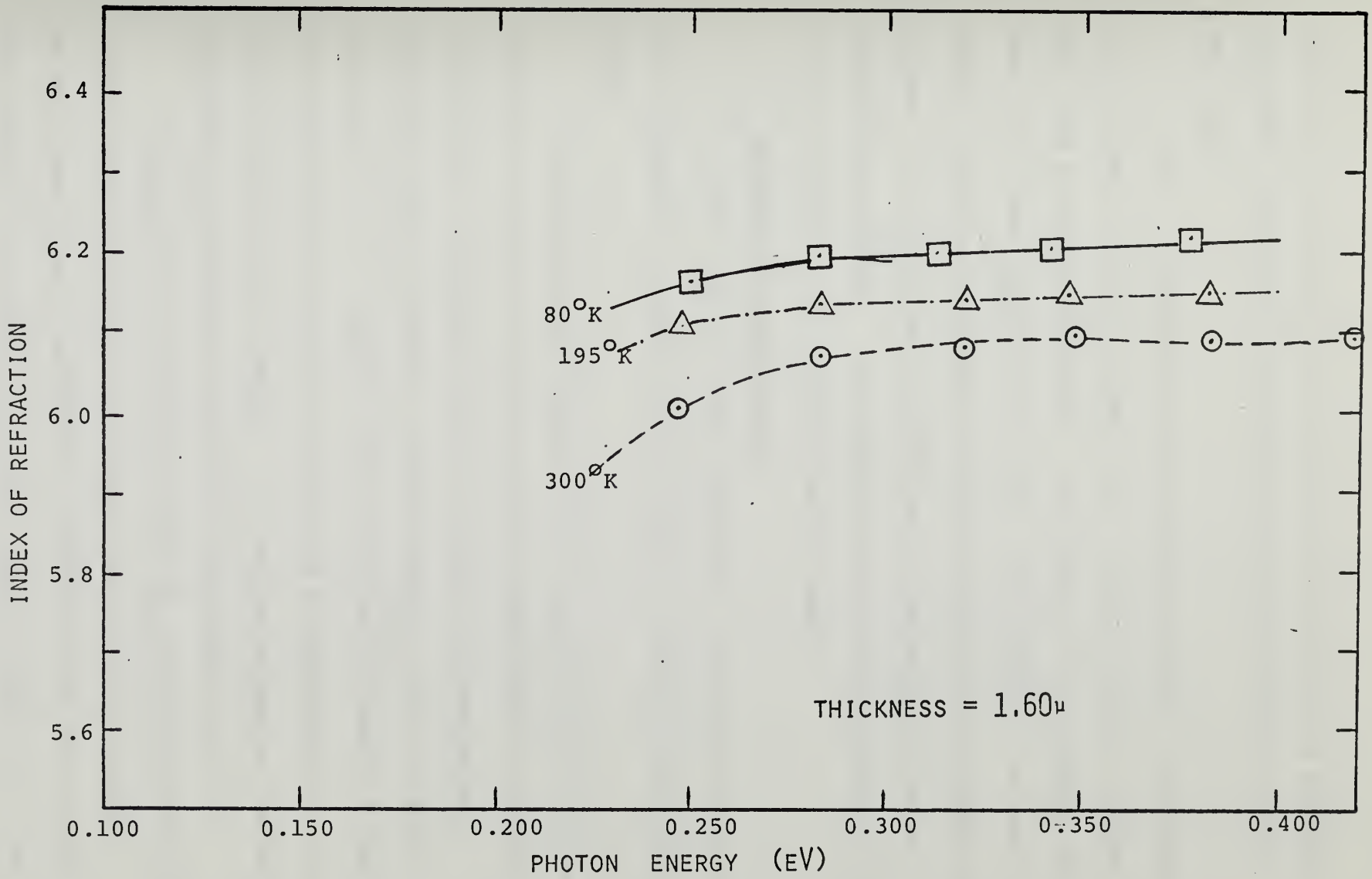

FIG. 4-2G - $PB_{0.15}SN_{0.85}TE$

gap as will be seen when the absorption coefficient data is presented. The index of refraction also increased as the mole-fraction of SnTe was increased.

Figure 4-3 compares the refractive index of PbTe films determined in this study with those of Zemel, et.al. [15] for similarly prepared thin films on rocksalt substrates. His values of n are slightly larger than the n values computed in this study. This difference no doubt is probably caused by the different method of thickness determination used by Zemel. His study used an interferometric and weighing technique to determine the thickness. This method does not account for the variation of film thickness across the entire optical sample.

2. The Absorption Coefficient

The other important optical constant is the extinction coefficient κ from which the absorption coefficient α is defined from Equation (2-17).

The absorption coefficient for the $Pb_{1-x}Sn_xTe$ thin films were determined from the R-T equations using the experimentally determined transmittance, reflectance, and film thickness, the independently determined index of refraction, and the refractive index of the KCl substrate [19, 20]. Numerical analysis based on the Rosenbrock iteration method [20] was applied in solving the R-T equations for κ and α using an IBM 360 digital computer. The computer program was checked by determining the absorption coefficients of well-known materials.

The absorption coefficients of thin $Pb_{1-x}Sn_xTe$ films determined in the fundamental absorption edge region are given in Figures 4-4. For each composition the absorption coefficient at 300, 195 and 80°K were obtained from analysis of a single carefully chosen film. The

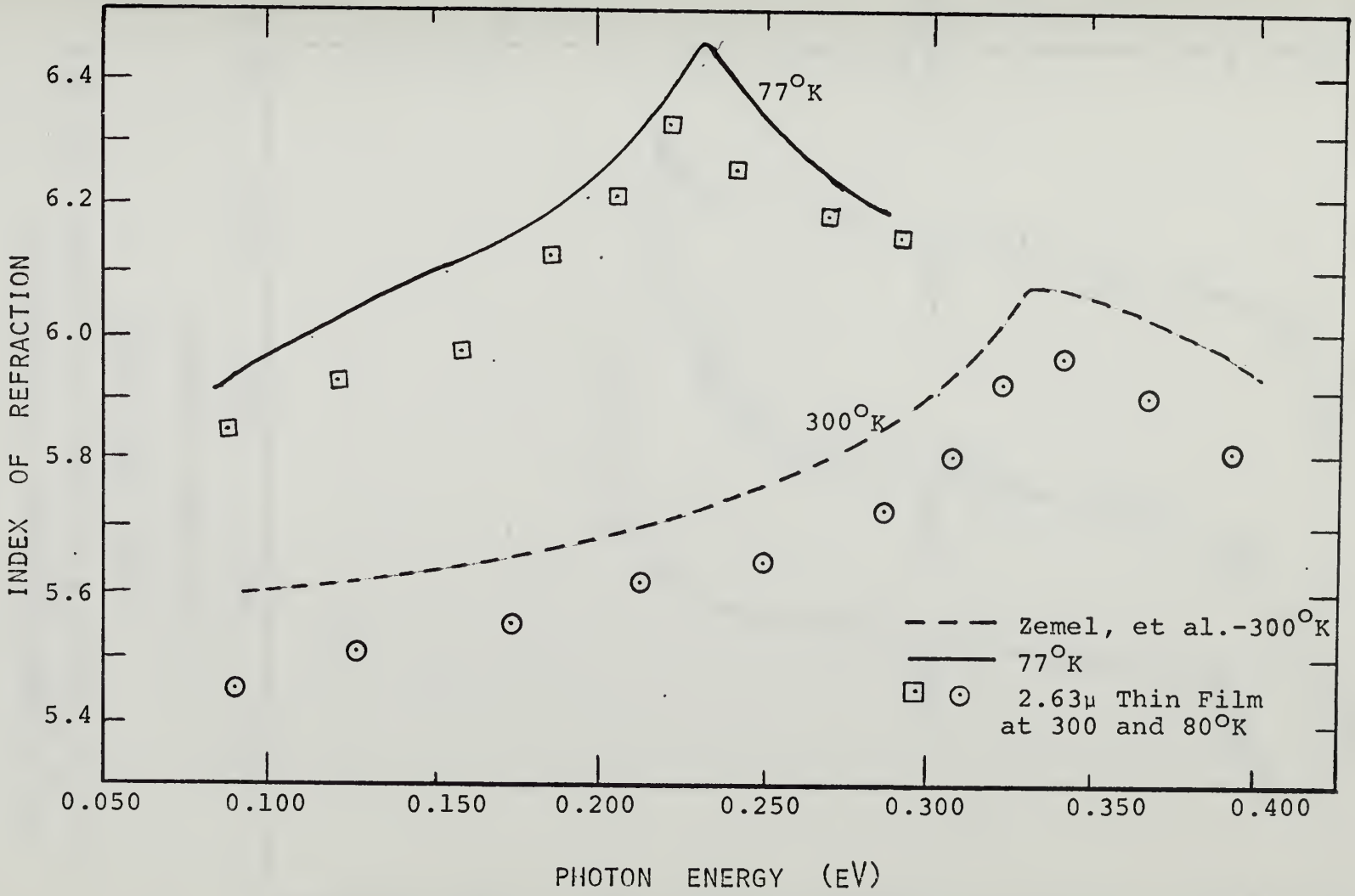

FIG. 4-3 - INDEX OF REFRACTION OF PbTe FILMS DETERMINED IN THIS WORK COMPARED WITH THOSE DETERMINED BY ZEMEL, ET.AL [15].

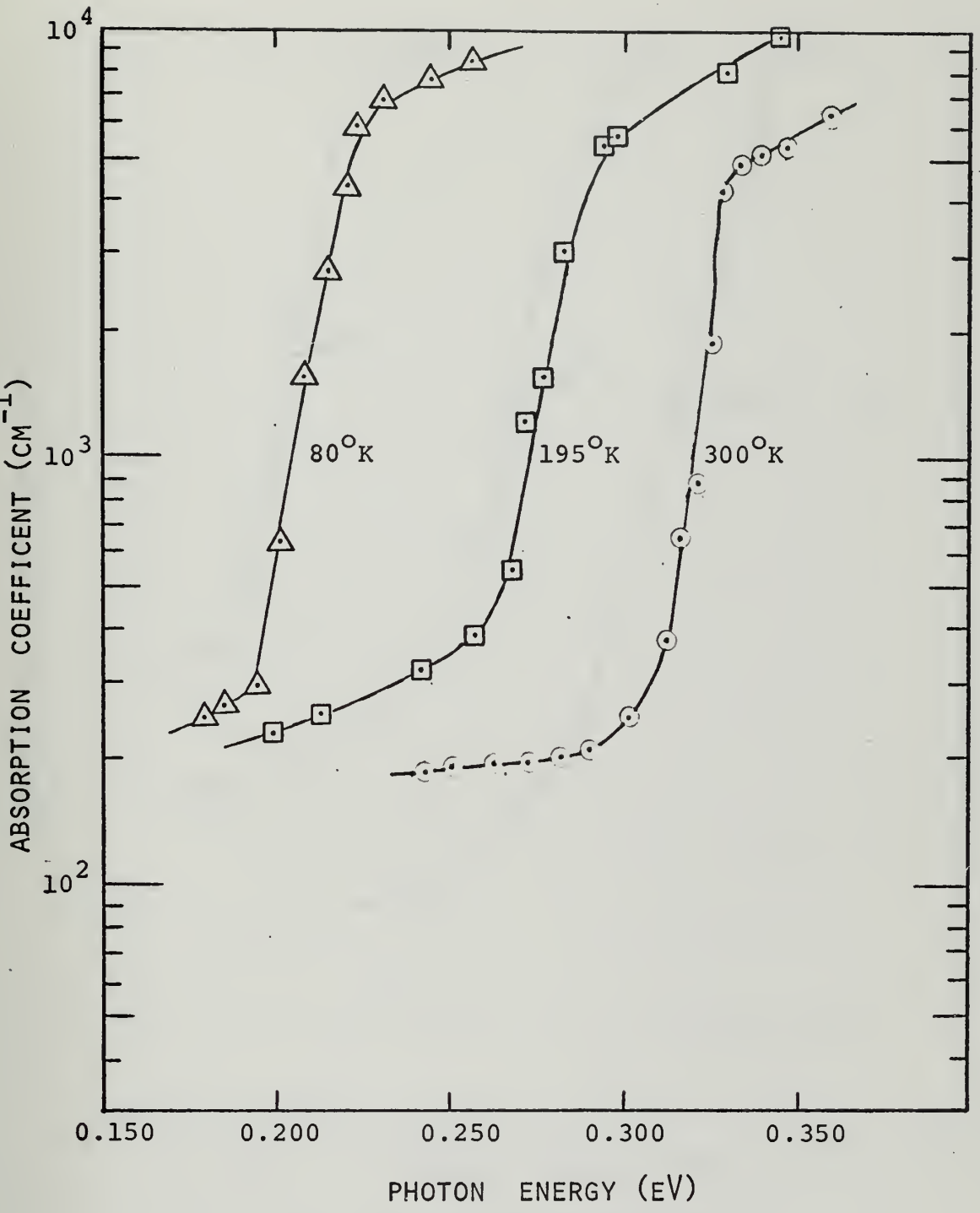

FIG. 4-4A - PBTE

FIG. 4-4 - ABSORPTION COEFFICENTS OF $PB_{1-X}SN_XTE$ IN THE FUNDAMENTAL ABSORPTION EDGE REGION.

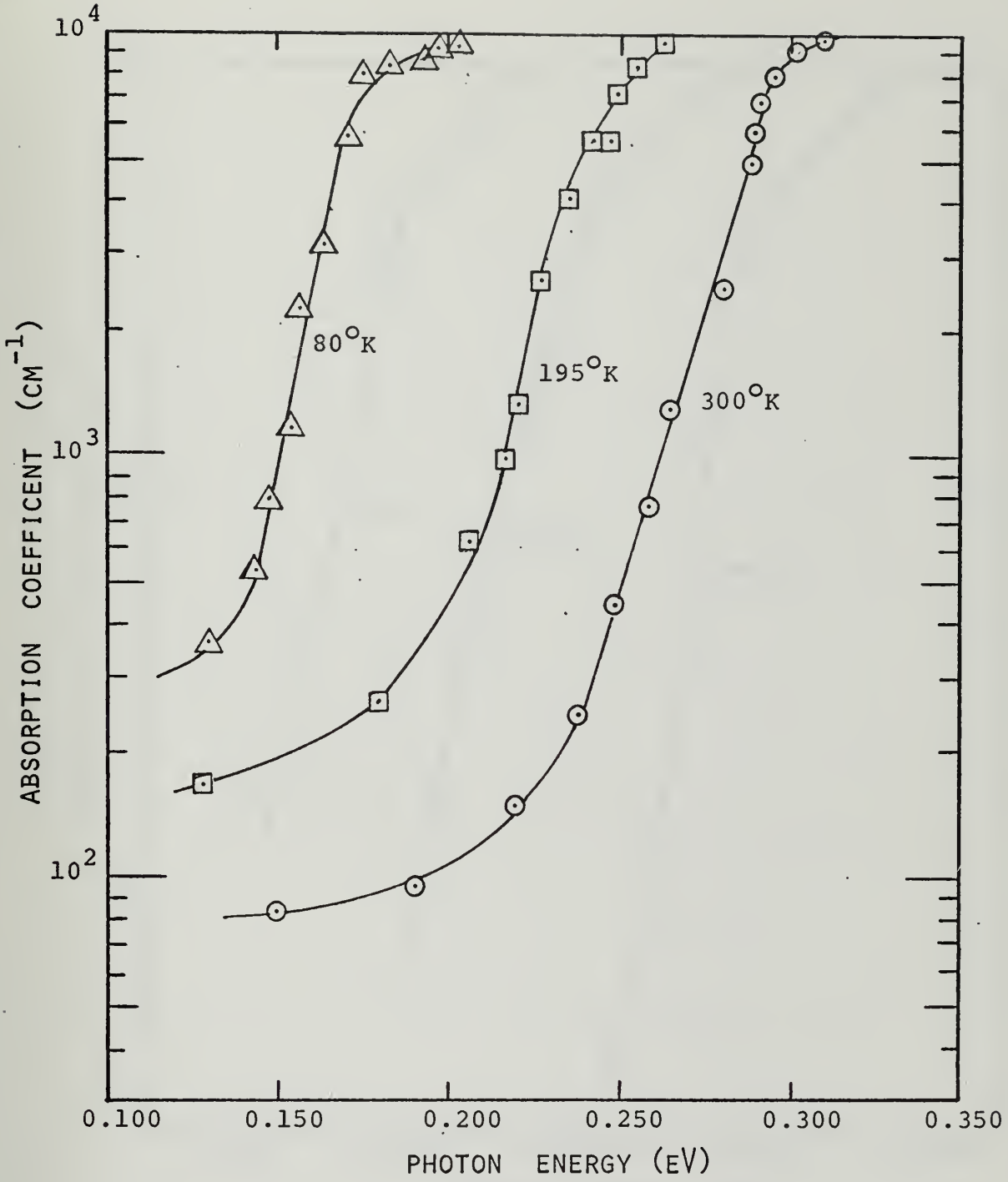

FIG. 4-4B - $PB_{0.94}SN_{0.06}TE$

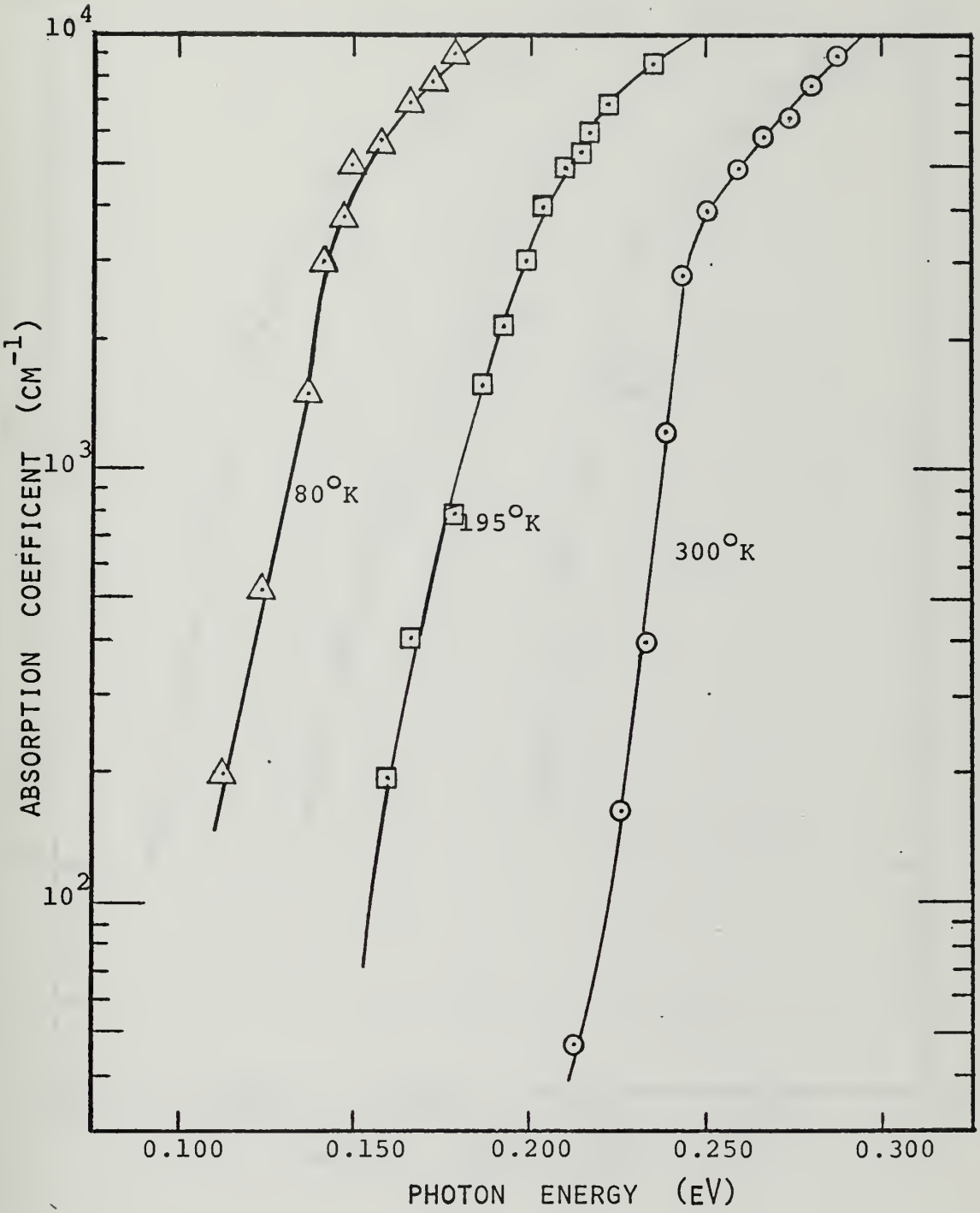

FIG. 4-4c - $Pb_{0.88}Sn_{0.12}Te$

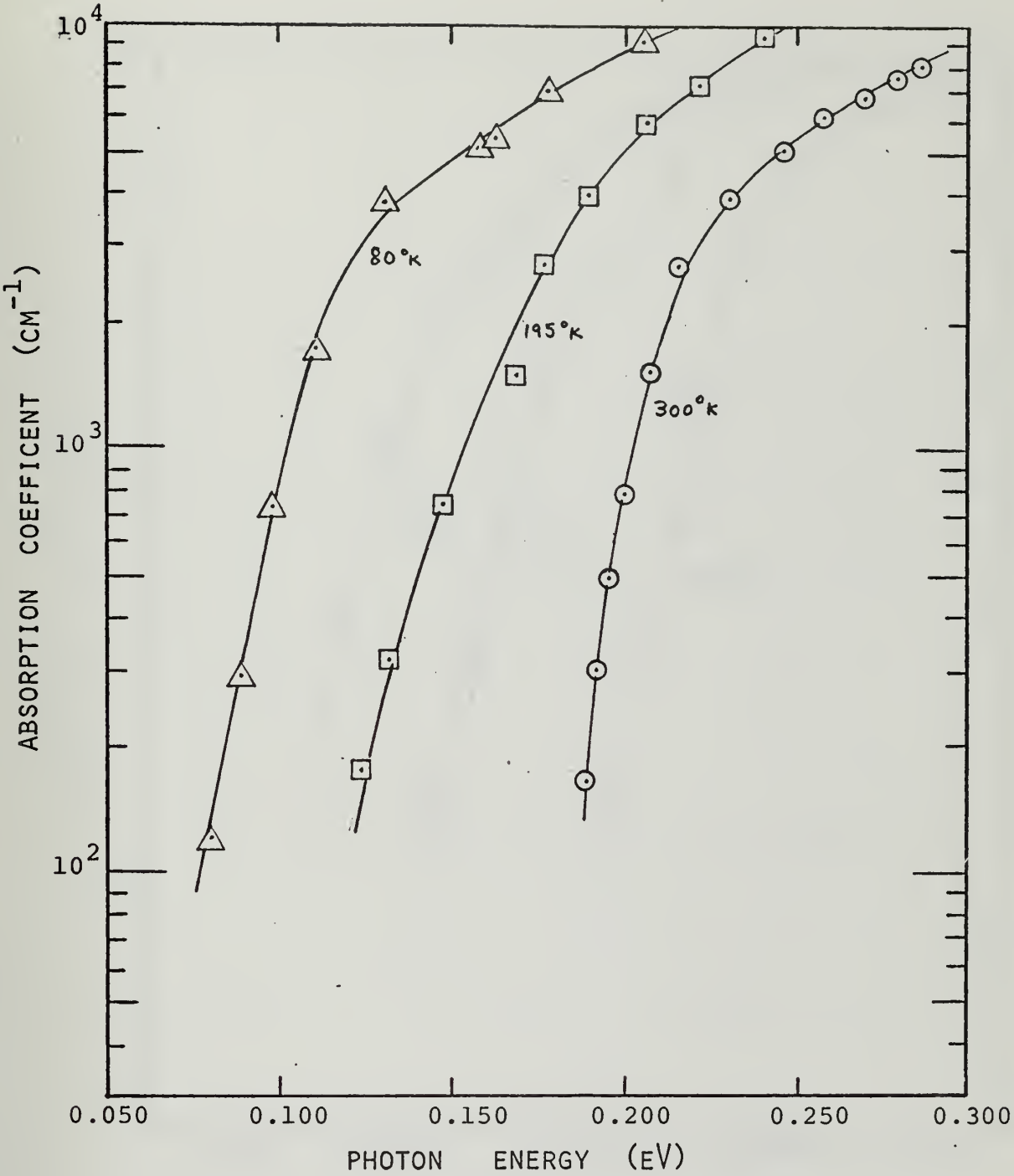

FIG. 4-4D - $PB_{0.82}SN_{0.18}TE$

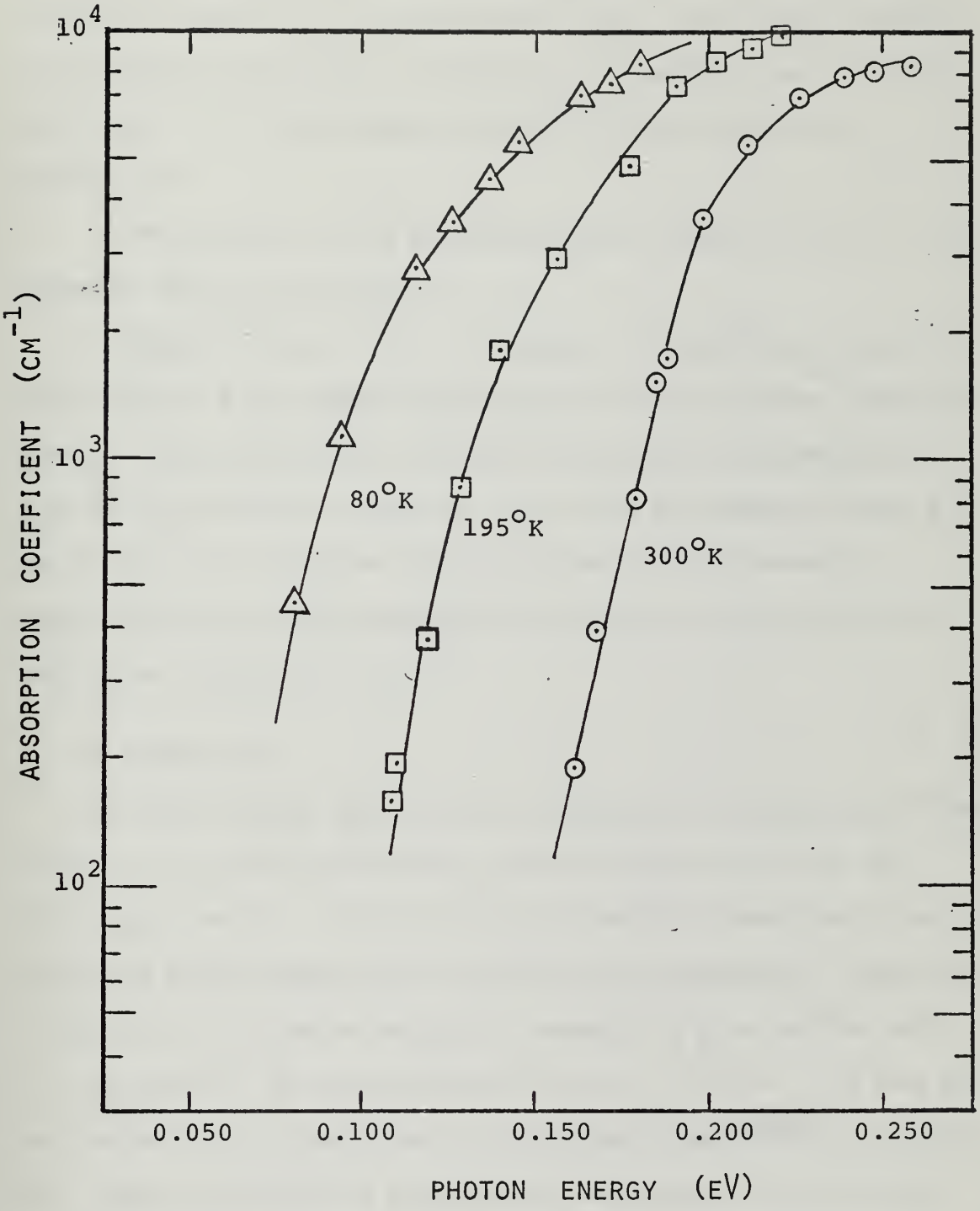

FIG. 4-4E - $PB_{0.76}SN_{0.24}TE$

position of the absorption edge and "knee" region were found to be essentially insensitive to uncertainties in R, T and n which were used in determining the absorption coefficient. Absorption spectra of PbTe determined in this study agree very well with those results of Scanlon [21].

The sharpness of the absorption edge in Figures 4-4 for $x \leq 0.24$ indicates direct gap transition.

Computer analysis for $x = 0.70$ and $x = 0.85$ did not result in the calculation of a pronounced edge because of the free-carrier absorption effects. The correspondence between the position of the absorption edge and the refractive index peak can be seen by comparing Figure 4-3 and Figure 4-4a. The absorption coefficient in the fundamental absorption edge region corresponded to low values of the extinction coefficient, typically $\kappa \leq 0.4$.

C. THE ENERGY GAP

The optical energy gap only was determined for the $Pb_{1-x}Sn_xTe$ films because of the limited absorption coefficient data as well as its inaccuracy above the α "knee" region which made it impossible to extrapolate the direct energy gap. The definition of the optical energy gap in which E_g is the photon energy corresponding to $\frac{\alpha}{2}$ was applied where α is the value of the absorption coefficient at the knee. The knee point was located by the intersection of the extrapolated absorption edge and the α curve just above the knee region. The values of α at the knee and $\frac{1}{2}\alpha$ are given in Table 4-1 along with the corresponding optical energy gap determined from the absorption data. The peak of the refractive index is also compared with the value of the optical energy gap. In all cases for $x \leq 0.24$, the peak of the refractive index

Table 4-1. Energy Gap Data of $Pb_{1-x}Sn_xTe$ at Various Temperatures.

x	T(°K)	knee x 10^{-3}	knee x 10^{-3}	Optical E_g(eV)	n peak (eV)
PbTe	300	4.7	2.35	0.325	0.330
	195	5.2	2.60	0.265	0.280
	80	6.4	3.2	0.230	0.235
0.06	300	8.0	4.0	0.280	0.290
	195	5.9	2.95	0.230	0.240
	80	7.5	3.75	0.165	0.175
0.12	300	3.7	1.85	0.245	0.255
	195	5.8	2.9	0.200	0.210
	80	6.0	3.0	0.145	0.150
0.18	300	4.0	2.0	0.220	0.235
	195	4.1	2.05	0.170	0.190
	80	3.4	1.7	0.120	0.140
0.24	300	6.2	3.1	0.195	0.200
	195	6.0	3.0	0.150	0.150
	80	4.0	2.0	0.115	0.120
0.70	Unable to Obtain this Data				
0.80					

occurred at a slightly higher photon energy than the optical energy gap. It was impossible to determine energy gap data for $x = 0.70$ and 0.85 since the free carrier absorption obscured the fundamental absorption edge.

The variation of the optical energy gap of $Pb_{1-x}Sn_xTe$ as a function of the mole-fraction of SnTe is given in Figure 4-5 using the energy gap values obtained from this optical absorption study along with previous data from laser emission, tunneling, and photovoltaic effect. The energy gap seems to obey a linear relation for $x \leq 0.24$ as indicated by the straight parallel lines. Magneto-optical studies on $Pb_{1-x}Sn_xTe$ suggest a slight non-linearity for large x. The lines in Figure 4-5 satisfy the equation:

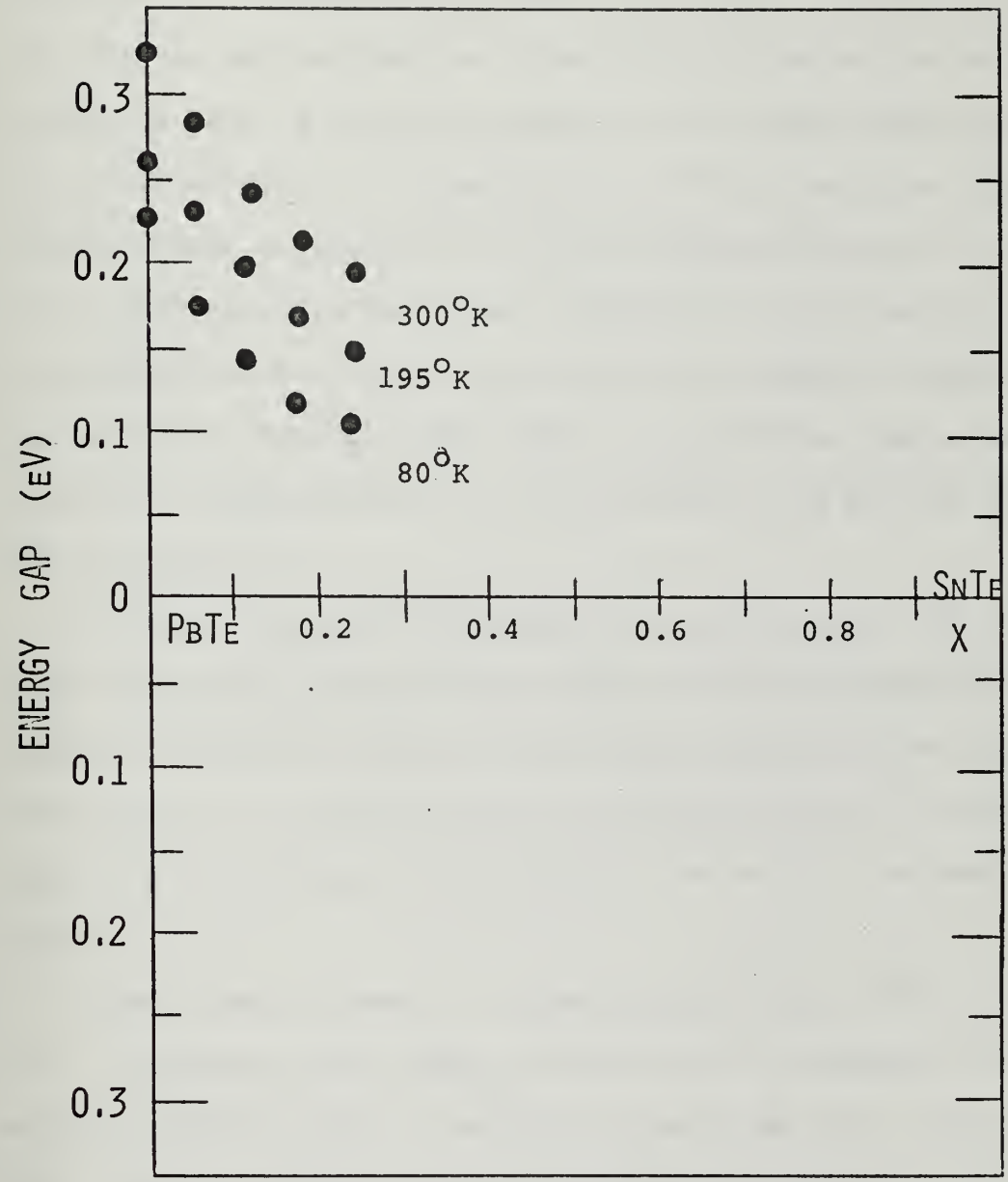

FIG. 4-5 - ENERGY GAP OF $Pb_{1-X}Sn_XTe$ AS A FUNCTION OF X, THE MOLE FRACTION OF SnTe DETERMINED EXPERIMENTALLY FROM OPTICAL ABSORPTION.

V. CONCLUSIONS

Index of refraction data and absorption coefficient data for compositions of $x \leq 0.24$ were determined by this study. Energy band inversion was not confirmed due to the high free-carrier concentrations for samples having a large mole-fraction of SnTe which effectively masked the absorption edge. For composition $x \leq 0.24$ the refractive index revealed a peak corresponding to the sharp absorption edge. For $x = 0.70$ and $x = 0.85$ the refractive index, affected by free-carrier absorption, was dependent on free-carrier concentration and showed no dispersion in the fundamental absorption edge region. No absorption edge values were computed for these concentrations which prevented the defining of the optical energy gap.

The index of refraction and absorption coefficients of $Pb_{1-x}Sn_xTe$ in the fundamental absorption edge region are results previously unavailable but appear consistent with expected behavior. The optical energy gap for $x \leq 0.24$ determined from optical absorption, complements energy gap data previously obtained from laser emission and photovoltaic cutoff.

Further study is needed for concentrations having a large value of x. A decrease in the number of free carriers is necessary to determine accurate optical constants and energy gap data. The use of metal-rich source material in the film deposition process is one method by which the reduction in free carriers may be accomplished.

BIBLIOGRAPHY

1. T.C. Harmen, A.R. Calawa, I. Melngailis, and J.O. Dimmock, Applied Physics Letters. Letter 11, 33 (1969)

2. Melngailis I. and Harman, T.C., Semiconductors and Semimetals, Vol. 5, Academic Press, 1970, p. 111

3. J.O. Dimmock, I Melngailis, and A.J. Strauss, Physical Review Letters, 16, p. 1193 (1966).

4. Nikolic, P.M., British Journal of Applied Physics, 16, p. 1075, (1965)

5. Esaki, L. and Stiles, P.J., Physical Review Letters, 16, p. 1108 (1966).

6. Strauss, A.J., Physical Review, 157, p. 608 (1967).

7. Conklin, J.B., Johnson L.E., and Pratt G.W., Physical Review, p. 1282 (1965).

8. Moss, T.S., Optical Properties of Semiconductors, Butterfield Scientific Publications, 1959.

9. Stern F., Elementary Theory of the Optical Properties of Solids, Solid State Physics, Vol. 15, Academic Press, 1963.

10. Lin, P.J. and Kleinman, Physical Review, 142, p. 478 (1966).

11. Heavens, O.S. Optical Properties of Thin Solid Films, Butterworths Scientific Publications, London, 1953.

12. Stratton, J.A., Electromagnetic Theory, pp. 496,513, McGraw-Hill, (1941).

13. Riedl, H.R. and Schoolar, R.B., Physical Review, 131, p. 2082 (1963).

14. Schoolar, R.B., and Dixon, J.R., Journal of the Optical Society of America, 58, p. 119 (1968)

15. Zemel, J.N., Jensen, J.D., and Schoolar, P.B., Physical Review, 140, p. 330 (1965).

16. Golovashkin, A.I., Soviet Physica, JETP 1, p. 38 (1960).

17. Riedel H.R., Dixon, J.R., and Schoolar, R.B., Physical Review, 162, p. 692 (1967).

18. Grant, P.M. and Paul, W., Journal of Applied Physics, 37, p. 3110 (1966).

19. Kohlrausch, F., Praktische Physik, Vol. 2, Teubner

20. Smakula, A., Einkristalle, Springer, (1962).

21. Scanlon, W.W., Physics and Chemistry of Solids, 8. p. 667 (1965).

INITIAL DISTRIBUTION LIST

		No. Copies
1.	Defense Documentation Center Cameron Station Alexandria, Virginia 22314	2
2.	Library, Code 0212 Naval Postgraduate School Monterey, California 93940	2
3.	Assc. Professor Tien F. Tao, Code 52 Tv Department of Electrical Engineering Naval Postgraduate School Monterey, California 93940	4
4.	Asst. Professor C. C. Wang, Code 52 Wf Department of Electrical Engineering Naval Postgraduate School Monterey, California 93940	1
5.	ENS Victor M. Walz USN 72 Via Havarre Merritt Island, Florida 32952	1

DOCUMENT CONTROL DATA - R & D

(Security classification of title, body of abstract and indexing annotation must be entered when the overall report is classified)

1 ORIGINATING ACTIVITY (Corporate author)
Naval Postgraduate School
Monterey, California 93940

2a. REPORT SECURITY CLASSIFICATION
Unclassified

2b. GROUP

3 REPORT TITLE
The Determination of Optical Properties and Energy Gap of $Pb_{1-x}Sn_xTe$ Thin Films in the Fundamental Absorption Edge Region

4 DESCRIPTIVE NOTES (Type of report and inclusive dates)
Master's Thesis (June 1972)

5. AUTHOR(S) (First name, middle initial, last name)
Victor Martin Walz, Jr.

6. REPORT DATE
June 1972

7a. TOTAL NO. OF PAGES
76

7b. NO. OF REFS
21

8a. CONTRACT OR GRANT NO.

b. PROJECT NO.

c.

d.

9a. ORIGINATOR'S REPORT NUMBER(S)

9b. OTHER REPORT NO(S) (Any other numbers that may be assigned this report)

10. DISTRIBUTION STATEMENT
Approved for public release; distribution unlimited.

11. SUPPLEMENTARY NOTES

12. SPONSORING MILITARY ACTIVITY
Naval Postgraduate School
Monterey, California 93940

13. ABSTRACT

The optical properties of single-crystal $Pb_{1-x}Sn_xTe$ thin films in the fundamental absorption edge region were investigated. Tin compositions of $0 \leq x \leq 0.24$, where x is the mole fraction of SnTe, were studied from room to liquid nitrogen temperatures. Two thin film samples with $x = 0.70$ and $x = 0.85$ were also studied in an attempt to confirm the inversion of the conduction and valence bands which had been previously predicted for this narrow-gap semiconductor. The index of refraction n and the absorption coefficient α were determined from transmission and reflection measurements made on films 0.8 to 5.0 microns thick, which were deposited on cleaved (100) faces of KCL rocksalt substrates. The optical energy gap was determined from the position of the absorption edge in the absorption spectrum.

The index of refraction was obtained using the interference fringe method. For $0 \leq x \leq 0.24$ a peak in n was observed. The index of refraction of films with a high Sn content exhibited free carrier absorption and free carrier concentration dependence. The absorption coefficient was calculated froman analysis of the theoretical reflectance R and transmittance T equations for a thin film on substrate model by using the experimentally determined R, T, and n values. The absorption spectrum showed relatively sharp absorption edges for $x \leq 0.24$ and broadened edges for higher Sn concentrations. Variations in the peak of the n spectra and the sharpness of the absorption edges were observed and accounted for.

DD FORM 1 NOV 65 1473 (PAGE 1)
S/N 0101-807-6811

Security Classification

A-31408

KEY WORDS	LINK A		LINK B		LINK C	
	ROLE	WT	ROLE	WT	ROLE	WT
$Pb_{1-x}Sn_xTe$ Optical Properties						
Absorption Coefficient						
Index of Refraction						
Optical Energy Gap						